Cold and hot atomic vapors: a testbed for astrophysics?

Quentin Baudouin, William Guerin, Robin Kaiser

Chapter 1

Cold and hot atomic vapors: a testbed for astrophysics?

Q. Baudouin, W. Guerin, and R. Kaiser

Institut Non Linéaire de Nice,
CNRS and Université Nice Sophia-Antipolis,
1361 route des Lucioles, 06560 Valbonne, France

Atomic physics experiments, based on hot vapors or laser-cooled atomic samples, may be useful to simulate some astrophysical problems, where radiation pressure, radiative transport or light amplification are involved. We discuss several experiments and proposals, dealing with multiple-scattering of light in hot and cold atomic vapors, random lasing in cold atoms and light-induced long-range forces, which may be relevant in this context.

1. Introduction

In the last two decades, the development of laser cooling of atoms and its subsequent use for generating degenerate quantum gases of dilute atomic vapors has already seen a number of applications, ranging from high-precision atomic clocks to fundamental studies related to condensed matter and quantum information technology.[1] All these applications are subject of intense research by numerous groups and are widely discussed in the literature.

In this chapter, we would like to point out the possible applications of cold-atom experiments and, more generally, of atomic-physics experiments, to another field, astrophysics. As a matter of fact, atomic physics has a century-long tradition of contributing to the knowledge and understanding of the universe by its contributions to understanding the atomic structure and to spectroscopy. It seems however that in the last decades, part of the atomic-physics community has lost most of its links with astrophysics. Here, we discuss some possible links between astrophysical problems or situations and modern atomic-physics experiments, especially with cold atoms.

2   *Q. Baudouin, W. Guerin, and R. Kaiser*

The most obvious link between astrophysics and cold-atom physics is probably the concept of radiation pressure. This force exerted by light is the basic tool for laser cooling and trapping of neutral atoms.[2] Besides the explanation given by Kepler for the tail of comets, radiation pressure is also one fundamental ingredient in stellar physics: light coming from the inside of stars contributes to counterbalance gravity and thus to prevent stars from collapsing. Interestingly, the same kind of equilibrium is at play in a magneto-optical trap (MOT) as soon as the number of atoms becomes large: as discussed in more detail later, the MOT size is governed by the balance between the trapping force (induced by radiation pressure from external laser beams) and the repulsive force induced by radiation pressure from light scattered from inside the sample. To be more precise, in both cases (stars and MOT), light inside the medium is in the *multiple scattering regime*, which is another unifying concept between astrophysics and cold atoms.

In astronomy, the systems are so huge in size (and also sometimes very dense) that the probability for light to cross the medium without being scattered is often very low: the medium is said to be opaque, its "optical thickness" to be large. For a cold-atom cloud, the density is very low and the sample is small, but this is compensated by strong resonances, which are not broadened by Doppler effects. The medium is also opaque, but only for a very narrow range of light frequency. In laboratory hot vapor, the Doppler effect weakens the transitions but it is easy to recover a large optical thickness by increasing the density. Thus, phenomena related to multiple scattering of light in stellar gases can be experimentally investigated in atomic-physics experiments, often with different orders of magnitude but usually in a simpler situation and with well-controlled and tunable parameters. This is relevant because the way astronomers obtain information about the universe is to detect light (or, more generally, electromagnetic waves). If the radiation has undergone multiple scattering, the original information may be blurred, and a precise understanding or simulation of the multiple-scattering process is necessary to access the interesting physical quantities. Laboratory experiments can thus serve as a testbed to compare the simulations with experiments. Furthermore, experiments can provide new ideas, either for new observed phenomena that could be searched for in space, or for novel detection techniques.

Therefore, the purpose of this chapter is to discuss several experiments involving multiple scattering of light in cold or hot atomic vapors, which we think may be interesting from an astrophysical point of view. Our

presentation is organized in three main parts. In the next section, we present experiments on light diffusion in cold atoms, demonstrating radiation trapping, and in hot vapors, showing that the Doppler effect makes light transport superdiffusive, with the occurrence of Lévy flights. In Sec. 3, we discuss the amplification of light by atomic vapors, which happens also in space,[3] and an experiment combining light amplification and multiple scattering, leading to a so-called "random laser". Finally, in Sec. 4, we discuss some mechanical aspects of multiple scattering in cold atoms, which creates long-range forces between atoms, with interesting analogies to astrophysical systems. Note that cold atoms are especially appropriate for studying phenomena involving light-induced forces because they are sensitive to very small forces. On the contrary, for phenomena involving the Doppler effect, frequency redistribution or collisions between gases of different species, hot atoms are more appropriate.

2. Light transport in atomic vapors

A diffusion equation for the propagation of light has been used as early as 1922 by Compton to describe the transport of light in an atomic vapor.[4,5] Soon afterwards, however, pioneering experiments by Zemansky on the decay of the fluorescence emitted by an initially excited mercury vapor have shown a deviation from the prediction of such a diffusion model.[6] It was then realized by Kenty that the frequency shift induced by scattering in a Doppler-broadened medium leads to lower excitation probabilities for photons with frequencies far from the center of the atomic resonance.[7] Indeed photons far from the atomic resonance can propagate over larger distances and the escape from a finite-size system cannot be described with a diffusion equation. Later, Holstein proposed an integro-differential equation to describe the transport of light taking into account the step-length distribution of the photons.[8] For photons at fixed frequency, this step-length distribution is an exponentially decreasing function, with well-defined mean free path and higher moments. For the diffusion model to fail, a divergence of the second moment of the step-length distribution is required. Kenty and Holstein showed that if the frequency of the photons inside the atomic vapor follows a gaussian distribution (motivated by the gaussian velocity distribution of the atoms) the step-length distribution of the photons has a divergent second moment, consistent with the observations of Zemansky.

A similar model was developed independently a few years later in the context of astrophysics to describe the radiative transfer in stellar atmo-

4   Q. Baudouin, W. Guerin, and R. Kaiser

spheres out of local thermal equilibrium.[9–11]

In this section, we investigate the case of light scattering in atomic vapors. In cold atoms, frequency redistribution can be neglected in most situations and light transport can be described by a diffusion equation. On the contrary, in room-temperature ("hot") vapors, frequency redistribution changes drastically the transport properties.

2.1. *Resonant scattering in cold atoms*

Some basics of multiple scattering in cold atoms can be found in[12] and some more evolved theoretical concepts in.[13,14] For this section, we only need to consider the atoms as point-like dipoles. Then, for a two-level atom probed by a weak, monochromatic laser, the elastic scattering cross-section is given by

$$\sigma_{\mathrm{sc}}(\delta) = \frac{\sigma_0}{1 + 4\delta^2/\Gamma^2}, \tag{1}$$

where δ is the detuning between the incident light and the atomic transition, Γ is the linewidth of the transition, and $\sigma_0 = 6\pi/k_0^2 = 3\lambda^2/2\pi$ is the on-resonance scattering cross-section, with $\lambda = 2\pi/k_0$ the wavelength of the transition [a]. All experiments discussed in this chapter have been performed with rubidium, with $\lambda = 780$ nm (D_2 line) and $\Gamma/2\pi = 6.1$ MHz. Another important quantity is the mean-free-path ℓ_{sc} between two scattering events, given by

$$\ell_{\mathrm{sc}} = \frac{1}{\rho\sigma_{\mathrm{sc}}}, \tag{2}$$

where ρ is the atomic density. Still considering only a weak probe beam and no external pump laser, there is no inelastic scattering nor absorption or amplification. The attenuation of the beam propagating in the medium is thus only due to elastic scattering, and the transmission T in a homogeneous sample of length L is given by

$$T = e^{-\rho\sigma_{\mathrm{sc}}L} = e^{-L/\ell_{\mathrm{sc}}}. \tag{3}$$

The quantity $b = \rho\sigma_{\mathrm{sc}}L = L/\ell_{\mathrm{sc}}$ is called the optical thickness and quantifies how much the medium is opaque, or diffusive. Typically, when $b \gg 1$, i.e. $L \gg \ell_{\mathrm{sc}}$, light is in the multiple-scattering regime. Obviously, a similar relation as Eq. (1) holds also for the optical thickness, and we often use the

---

[a]Note that for a scalar model, the scattering cross section is given by $\sigma_0 = \lambda^2/\pi$. When taking into account the polarization of the light, one has the well known relation $\sigma_0 = 3\lambda^2/2\pi$.

on-resonance optical thickness $b_0 = \rho\sigma_0 L$ of the optical cloud to characterize the diffusive power or the "size" of our sample. Equation (1) shows immediately an important advantage of working with cold atoms, namely the ability to change the scattering cross-section by simply detuning the probe laser from a few megahertz. In particular, it allows us to measure the on-resonance optical thickness from a transmission spectrum even if this optical thickness is very high.[15]

2.2. *Normal diffusion in cold atoms*

Random walk of particles in a disordered medium is often well described by a diffusion equation, characterized by a linear increase in time of the mean square displacement of the particles: $\langle r^2 \rangle = Dt$, with D the diffusion coefficient. One assumption for the diffusion equation to hold is that the size ℓ of each step of the random walk follows a probability distribution $P(\ell)$ with a finite second moment $\langle \ell^2 \rangle$, allowing the application of the central limit theorem.

Considering photons undergoing only elastic scattering off atoms at rest, the distribution of the step length between two scattering events is exponential, i.e.,

$$P(\ell) \propto e^{-\ell/\ell_{\rm sc}}, \tag{4}$$

where $\ell_{\rm sc}$ is the mean free path, as defined above. The condition to apply the central limit theorem is fulfilled and, after a large number of steps, the light-intensity (or energy density) distribution in the medium converges towards a Gaussian distribution whose width increases linearly with the square root of time. This process is described by the diffusion equation (without source nor absorption/amplification in the medium)

$$\frac{\partial W(\mathbf{r}, t)}{\partial t} = D\nabla^2 W(\mathbf{r}, t), \tag{5}$$

where W is the energy density, v is the transport velocity inside the medium, and D is the diffusion coefficient given by

$$D = \frac{v\,\ell_{\rm t}}{3}\,, \tag{6}$$

with $\ell_{\rm t}$ the transport length. The transport length is related to the mean free path by

$$\ell_{\rm t} = \frac{\ell_{\rm sc}}{1 - \langle \cos\theta \rangle}, \tag{7}$$

6   *Q. Baudouin, W. Guerin, and R. Kaiser*

where $\langle\cos\theta\rangle$ is the average cosine of the scattering angle. Since we will consider only Rayleigh scattering in the following, we take $\langle\cos\theta\rangle = 0$ and $\ell_{\mathrm{t}} = \ell_{\mathrm{sc}}$.

2.2.1. *Diffuse transmission and reflection*

A first characterization of light diffusion in cold atoms can be obtained in a static experiment, by measuring the diffuse transmission and reflection,[15] see Fig. 1. It shows in particular that the diffuse transmission decreases much more slowly than the exponential attenuation of the ballistic (or coherent) beam, as expected from the diffusion equation.[16] This can have practical consequences when one needs to evaluate the light reaching the edges of the cloud, e.g., for imaging purposes. The dominant contribution can be the diffuse transmission, which thus should not be neglected. In this experiment, the optical thickness is changed by detuning the probe laser, illustrating the advantage of having a narrow resonance.
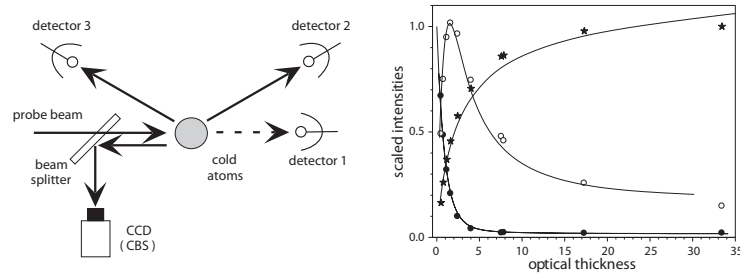

Fig. 1.   Left: Experimental scheme for measuring diffuse transmission and reflection. A small collimated laser beam is sent onto a cold-atom cloud. Three detectors measure the ballistic intensity, the diffuse reflection and the diffuse transmission. Right: the ballistic transmission (black circles) follows a Beer-Lambert law (exponential decrease). The diffused reflection (black stars) increases with the optical thickness. The diffused transmission (white circles) is not monotonic with the optical thickness. For large optical thickness b it evolves as $1/b$. Adapted from.[15]

2.2.2. *Radiation trapping with two-level atoms*

Another experimental situation probing multiple scattering of light consists in a time-dependant detection of the scattered light (see Fig. 2).[8,17] Such radiation trapping in cold atoms has been first demonstrated in,[18] where decay times of atomic fluorescence beyond the lifetime of the excited
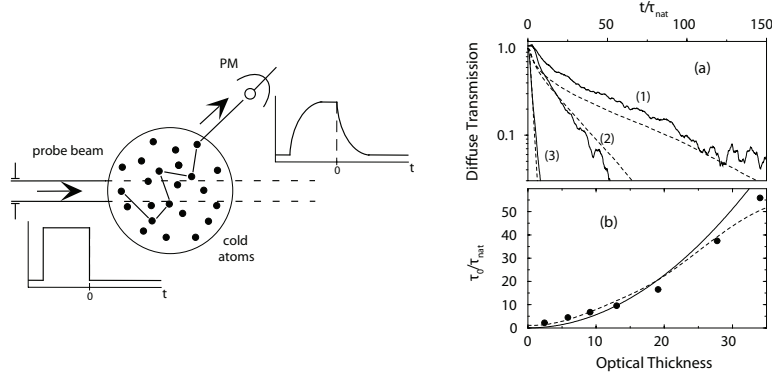
Fig. 2.   Left: Experimental scheme for observing radiation trapping. A small collimated laser beam is sent onto a cold-atom cloud. A photomultiplier (PM) records the fluorescence signal. At time $t = 0$, the laser is switched off. Right: Temporal trace of the decreasing fluorescence (a), and the corresponding time constants as a function of the optical thickness (b). Adapted from.[19]

state for single atom scattering has been observed with increasing optical thickness.

In Ref.,[19] we have shown that the transport time τ, which is the sum of the scattering time at each atom t_{sc} and propagation time between two scattering events t_{prop}, is independent of the laser detuning, as previously predicted[13] for scattering using narrow resonances. Note that this result is in contrast to the result of non resonant scattering, where the energy velocity of the light is constant. For cold atoms, the time between two successive scattering events is constant independent of the atomic density and thus of the average distance between scattering events.

This result can be used to obtain scaling laws for radiation trapping in cold atomic vapors. As $|kv| \ll \Gamma$, one typically neglects frequency redistribution during multiple scattering and one can thus assume a random walk of photons before radiation escapes the atomic system. For a Gaussian random walk, we have $\langle r^2 \rangle = Dt$. The average number of scattering events for transmitted photons is the ratio between the time spent in the system and the scattering time :

$$\langle N_{sc} \rangle = \frac{t}{\tau} = \frac{\langle r^2 \rangle}{D\tau}, \tag{8}$$

with $D = \ell_{sc}^2/(3\tau)$. When $\sqrt{\langle r^2 \rangle} \sim L = b\ell_{sc}$, the radiation can escape the system, leading to $\langle N_{sc} \rangle \sim 3b^2$. Radiation trapping times are thus expected to scale as b^2. However, as shown in,[20] the finite, non zero, temperature of

8   *Q. Baudouin, W. Guerin, and R. Kaiser*

laser-cooled atoms leads to a reduction of the trapping time, an indication that the Doppler effect is not completely negligible.[20,21] As we will show below, for hot atomic vapors ($|kv| \gg \Gamma$), the more important frequency redistribution leads to a novel regime of multiple scattering of light, described as Lévy flights.

2.2.3. *Radiation trapping with multilevel atoms*

In the experiments above, the atom laser detuning has been chosen such that a closed atomic transition is excited, making a description of light scattering by two-level atoms an excellent approximation (despite the more complex Zeeman substructure of these states[22–24]). Neglecting interference effects (considered not to be dominant, except for specific cases such as coherent backscattering[25] or for photon localization[26,27]), one can model radiation trapping by a transport equation of light coupled to equations for the atomic degrees of freedom. The simplest model for the atomic evolution is a set of rate equations for atoms and a diffusion equation for the light transport. Alternatively, one can use a more precise radiation transfer equation (RTE) to describe incoherent propagation of light including lower scattering orders and optical Bloch equations (OBE) for the atomic evolution.

Radiation trapping in atomic vapors is an important feature in many astrophysical situations. However, in this context, one rarely is in the presence of the required excitation spectra for closed atomic transitions to be excited. It is thus important to understand to what extent open transitions alter radiation trapping of light in atomic vapors. In recent experiments, we have extended our study of radiation trapping in a collection of cold atoms to open transitions, including four atomic levels (two ground states and two excited states), excited by two separate lasers.[28] In this configuration, each transition is driven by one laser and can be considered as a two-level subsystem. The two subsystems are then coupled to each other via spontaneous emission and by the trapped radiation.

In this experiment we have specifically studied the fluorescence of the atomic cloud as a function of the optical thickness. Keeping the number of atoms constant, any increase of the fluorescence of the cloud when changing the optical thickness is a collective effect and not merely the sum of N independent atoms. In this setup we have obtained atomic clouds with up to 10^{10} atoms and an optical thickness between 20 and 75. We illuminate the sample with two beams, called pump and repumper (Fig. 3(a)). The scat-

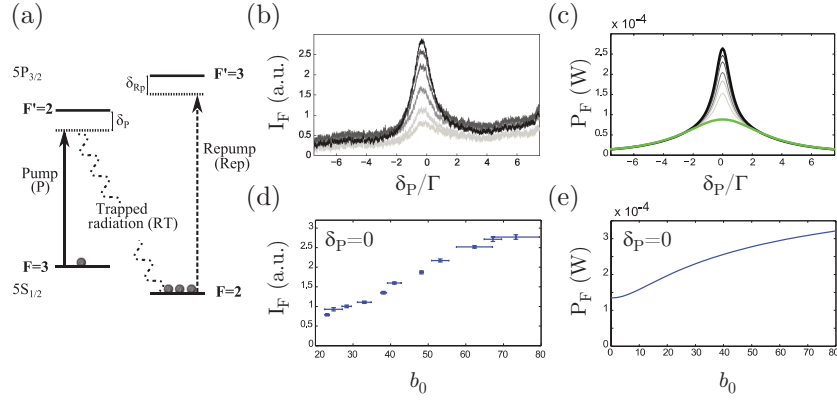*Cold and hot atomic vapors: a testbed for astrophysics?*   9

Fig. 3.   Radiation trapping with multilevel atoms. (a) Scheme of the atomic levels and lasers. (b) Detected fluorescence around the $|2\rangle \rightarrow |2'\rangle$ transition for different optical thickness. (c) Corresponding numerical simulation. (d) Amplitude of the fluorescence resonance as a function of the optical thickness. (e) Corresponding numerical simulation. Adapted from.[28]

tering of the pump produced photons coupling the "two two-level systems". If the pump is tuned close to the $F = 3 \rightarrow F' = 2$ resonance, the scattered light on the $F' = 2 \rightarrow F = 2$ line can be multiply scattered due to the large optical thickness. This trapped radiation will change the population ratio of the two ground states and so it will change the fluorescence emitted by the cloud, as scattering rates are not identical for atoms in the two ground states. An intuitive explanation for the impact of radiation trapping in this situation is to consider the trapped radiation as an additional repumper, shuffling the atoms into the $F = 3$ hyperfine level. The steady state population is thus affected compared to the independent-atom case (with only an external laser repumping atoms back into $F = 3$) leading to a subsequent modification of scattering by the pump laser.

Using rate equations for the atomic evolution with two external lasers and an incoherent pump for the trapped radiation, we can compute the steady state populations of the various atomic levels and the emitted light from the cloud, reproducing remarkably well the experimental results (see Fig. 3). Using rate equations for the atomic evolution obviously neglects interference effects such as electro-magnetically induced transparency (EIT). Usually such EIT features are observed when two external lasers excite a common excited state. In our situation, self-induced EIT might appear when the radiation trapping acts as the second coherent excitation to a
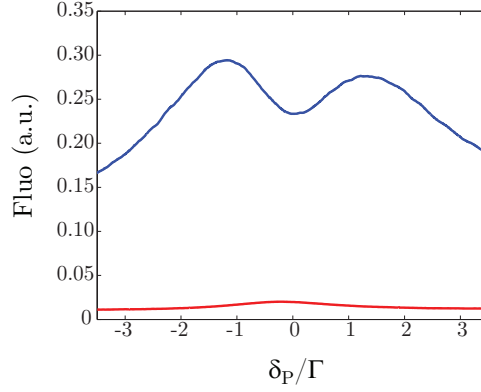
Q. Baudouin, W. Guerin, and R. Kaiser

Fig. 4.   Fluorescence of the cloud for small (red line) and large (blue line) optical thickness as a function of the pump detuning (see Fig. 3). Here the optical thickness is varied by changing the repumper intensity and keeping the pump intensity constant. The central dip at high optical thickness might be due to electromagnetically-induced transparency induced by the light trapped in the cloud by multiple scattering.

common atomic level in the excited state. In contrast to typical EIT experiments, where a pump laser frequency is kept fixed as a probe laser frequency is scanned across the two-photon resonance condition, in our experiment, the probe laser is self-generated and stays close to the two-photon resonance. Using a lower pump intensity than in[28] we have observed features unexplained by our rate equation model (Fig. 4), which might be explained by self-induced EIT, but a more precise analysis also taking into account diffuse forward and backward scattering is required. We speculate that such coherent features induced by radiation trapping can also occur in astrophysical systems, in the absence of two independent coherent laser excitations.

2.3. *Lévy flights in hot atomic vapors*

When the step-size distribution $P(\ell)$ is not exponential but follows an asymptotic power law $P(\ell) \sim 1/\ell^{\alpha}$, the moments of the distributions can become infinite. It has been long established that for $\alpha < 3$, the average square displacement is governed by rare but large steps[29] (Fig. 5). Such a class of random walk is called Lévy flights, corresponding to a superdiffusive behavior, where $\langle r^2 \rangle = Dt^{\gamma}$, with $\gamma > 1$. The broad range of applications of Lévy flights includes biology, economics, finance, catastrophe management and resonance fluorescence in astrophysical systems and atomic va-

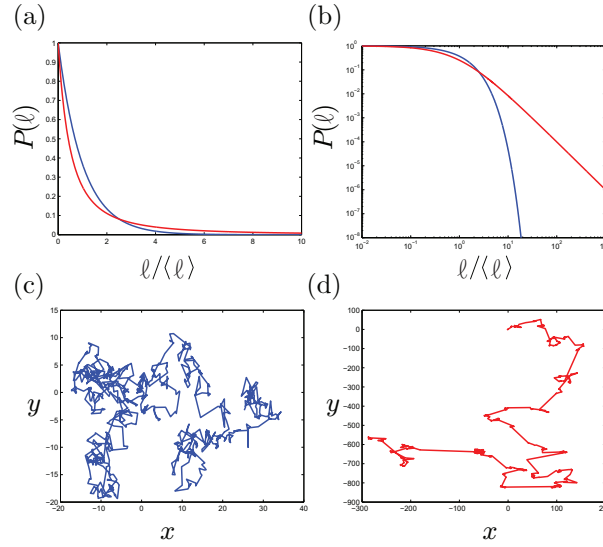*Cold and hot atomic vapors: a testbed for astrophysics?*   11

Fig. 5.   Top: Step size distribution $P(\ell)$ in linear scale (a) and in log-log scale (b) for the diffusive case (blue) $P(\ell) = \frac{1}{\ell_{sc}} e^{-\frac{\ell}{\ell_{sc}}}$ and for the Lévy case (red), we have plotted $P(\ell) = \frac{1}{(1+\ell)^2}$. Bottom: Examples of trajectories computed in two dimensions with a Monte-Carlo method for normal diffusion (c) and Lévy flights (d).

pors.[30–33] Large (non Gaussian) fluctuations also play a fundamental role in many physical situations, in particular around phase transitions, which has triggered considerable efforts to understand universal features of such phenomena.[34,35]

With light, superdiffusive behavior has been studied recently in engineered optical material,[36] but it has also been known for a long time to occur in the context of radiation trapping in hot atomic vapors. Because this phenomenon occurs in many different systems, ranging from stars[37] to dense atomic vapors[17] such as gas lasers, discharges and hot plasmas, this field has been subject to intense studies for many decades, including seminal work by Holstein.[8] It has been realized very early[7] that frequency redistribution has a profound impact on the multiple scattering features of light.

The system that we have considered is a room-temperature vapor of rubidium. In this system, the important Doppler shifts lead to frequency redistribution at the origin of Lévy flights. Here will will describe two experimental protocols we have implemented to characterize these Lévy

12   *Q. Baudouin, W. Guerin, and R. Kaiser*

flights.

2.3.1. *Qualitative analysis*

The description of multiple scattering of light in hot atomic vapors resulting in Lévy flights can be obtained using different assumptions.[8,17,38] An intuitive description of how Lévy flights can appear in inelastic scattering is to realize that for each frequency component, the scattering cross section $\sigma(\omega)$ can be associated to a scattering mean free path $\ell_{sc}(\omega)$ and a corresponding exponential distribution for the distance ℓ how far such a photon will propagate before scattering:

$$P(\ell, \omega) = \frac{1}{\ell_{sc}(\omega)} e^{-\frac{\ell}{\ell_{sc}(\omega)}}. \tag{9}$$

If the frequency spectrum of the light propagating in the atomic vapor is monochromatic (as it is to a good approximation for cold atoms), the step size distribution is an exponential and both the mean free path and the second moment of the step size distribution $\langle \ell^2 \rangle$ are finite. The central limit theorem thus applies and one can describe the multiple scattering process by a diffusion equation. However, when the frequency spectrum $\Theta(\omega)$ is broad, such that there is a strong variation of the decay length $\ell_{sc}(\omega)$, then the step size distribution averaged over the frequencies can significantly differ from an exponential and correspond to a power law. One can summarize this effect by saying that it is possible to have $\langle f(\omega) e^{-x(\omega)} \rangle_\omega \sim 1/x^\alpha$ with the appropriate $f(\omega)$.

More rigorous descriptions of this effect can be given. A first approach consists in using a radiative transfer model, including in the absorption cross section the natural (homogeneous) linewidth of the atomic transition and the frequency change at scattering, which depends on the scattering angle. A simplified version consists in neglecting the homogeneous linewidth. Assuming furthermore that there is no correlation between the frequencies after successive scattering events (complete frequency distribution - CFR), one can even derive an analytical expression of the step size distribution, which scales close to $P(\ell) \sim 1/x^2$. Once a step size distribution is obtained, one can perform a Monte Carlo simulation of the random walk of the photons through a slab and compute macroscopic properties such as the total diffuse transmission or the intensity profile of the light at the exit surface of the slab. Both the microscopic step size distribution and the macroscopic observables can also be obtained numerically without assuming CFR or neglecting the homogeneous linewidth. We note that in

contrast to specifically designed Lévy glass,[36,39] there are no correlations between the location of the scattering and the step size distribution.[40] We are thus closer to an annealed than a quenched disordered system.[41] Also, we have not introduced a truncation of minimum or maximum step sizes and are thus only limited by the finite size of the sample.

2.3.2. *Microscopic evidence of Lévy flights*

A direct measurement of the step size distribution of a photon is not an easy task. Indeed, in contrast to particle image velocimetry or other tracer methods (using e.g. radioactive labeling), no such labeling is possible with photons. It thus seems impossible to follow a photon and measure how far it travels before changing its direction inside a large system such as a star or a large cloud of atoms. In order to access the microscopic step size distribution of photons, we have designed a specific experimental geometry circumventing this apparently unsolvable problem. Indeed using the configuration of Fig. 6, we have been able to measure how far a photon travels in an observation cell with a low optical thickness.[42] In this cell, single scattering is dominant (necessary corrections by higher order scattering in this probe cell are discussed in[43]). The modification of the spectrum of the light entering this observation cell has been obtained via one or two scattering cells,[42] or - for calibration - using a monochromatic laser beam. When using scattering cells, the frequency of the light entering the observation

Fig. 6.   Left: Experimental setup used to measure the microscopic step-size distribution $P(\ell)$. Photons are scattered in a source cell and probed in an observation cell allowing the measurement of $P(\ell)$. Right: Step-size distribution $P(\ell)$ plotted in log-log scale. For an incident monochromatic laser beam (crosses), $P(\ell)$ shows an exponential decrease (fitting dashed line). For an incident Doppler-broadened light originated from a first scattering cell (dots), $P(\ell)$ has a power-law decrease (fitting dashed line). The continuous line comes from a microscopic model without any free parameter except the vertical scale. Adapted from.[42]

14   *Q. Baudouin, W. Guerin, and R. Kaiser*

cell has acquired the Doppler broadening as in large clouds of atoms and
we measure the step size distribution of photons leaving the preparation
cells. In Fig. 6, we show the measured step distribution for a monochro-
matic spectrum (blue exponential line). When using the preparation cell,
the step size distribution is a power law (green line) with $\alpha = 2.41$. A
multiple cell arrangement has been used to make sure that the detected
photons have no reminiscent memory effects as could occur with only a sin-
gle scattering at right angle. The Lévy exponent after multiple scattering
has been measured to be $\alpha = 2.09 \pm 0.15$.[42,44] For values of α below 3, the
second moment of the step size distribution diverges, entering the regime
of Lévy flights.[45]

2.3.3. *Macroscopic evidence of Lévy flights*

Despite the precise results obtained by the microscopic evidence of Lévy
flights in atomic vapors and the possible extension to adapt this scheme to
a larger variety of conditions relevant to astrophysics (including collisional
broadening, magnetic fields or large intensities), the multiple-cell geometry
has some practical limitations, mainly due to the small number of detected
photons. This leads to integration times of up to 30 hours, with images close
to the shot noise limit and requiring corrections due to cosmic rays.[42,44] We
have therefore changed our detection scheme by analyzing the total diffuse
transmission and the radial profile of light at the exit face of the sample.[36]

We illuminate a "camembert"-shaped cell (realizing a slab geometry)
with a low intensity laser, tuned to the resonance of the D_2 line of ^{85}Rb
(Fig. 7). This cell is inside an oven which allows the temperature to be
varied between $20°C$ and $200°C$. A temperature rise slightly increases the
Doppler broadening (the spectral width increase in $\sqrt{T}$) but the Rubidium
density increases sharply due to the almost exponential behavior of vapor
pressure with temperature. The opacity of the cell is measured by scanning
the frequency around the 4 absorption hyperfine transitions around the D_2
line of Rubidium. A fit of the hyperfine structure provides the opacity of the
system. Note that here we distinguish opacity $O(\omega)$ from optical thickness
$b(\omega)$. Both quantities are proportional to the atomic density ρ and length
of the cell L. The opacity is defined as $O = \rho\sigma(\omega)L$, where $\sigma(\omega)$ is the scat-
tering cross section neglecting the Doppler broadening, whereas the optical
thickness is the measured attenuation of the coherent forward beam, which
can be obtained from the opacity using an adequate convolution with the
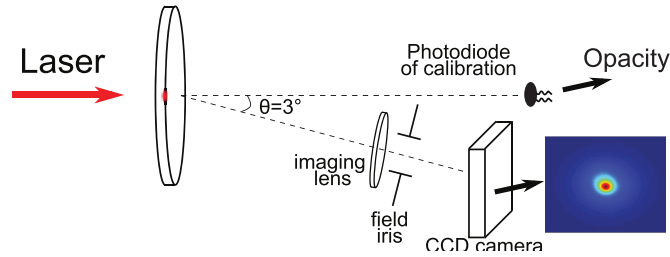Doppler broadening. To some extent, the opacity is the optical thickness

Cold and hot atomic vapors: a testbed for astrophysics?   15

Fig. 7.   Experimental setup to measure total output versus the optic $T(O)$ and the radial profile of transmitted intensity $P(r_\perp)$.

one would obtain if all atoms in the cell were laser-cooled with negligible Doppler broadening. The diffuse transmission and radial profile are then measured with a CCD camera imaging the cell. Using this detection protocol, we have been able to obtain macroscopic evidence of Lévy flights using images obtained with exposure times below one second.[46] The total diffuse transmission can also be monitored using fast photodetectors, allowing one in principle to investigate time dependent features such as Lévy walks. It is also possible to analyze the detected light for its polarization, allowing a direct comparison to numerical codes used in astrophysics for the detection of weak magnetic fields of the sun.[47]

As a first important calibration experiment, we have measured the total diffuse transmission across a slab of hot atoms and compared the extracted Lévy exponent to the one obtained via our microscopic detection scheme
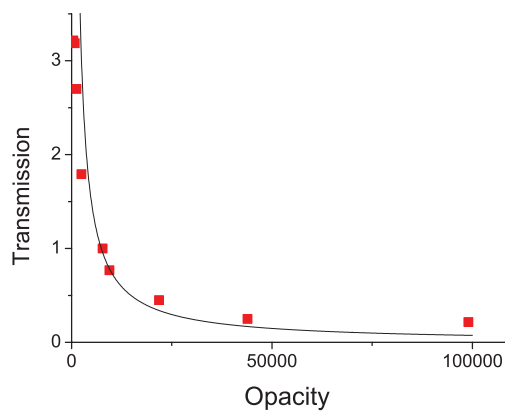

Fig. 8.   Total transmission as a function of opacity. A power law fit to the experimental data yields a Lévy exponent of $\alpha = 2.1$.

16   *Q. Baudouin, W. Guerin, and R. Kaiser*

of the step size distribution. For the total diffuse transmission, one expects in the case of Lévy flights a scaling as

$$T_{\text{Levy}} \propto 1/L^{(\alpha-1)/2}, \tag{10}$$

to be compared to Ohm's law of photons in the diffusive regime, where one has

$$T_{\text{diff}} \propto 1/L. \tag{11}$$

As shown in figure 8 we observe a clear deviation from Ohm's law for the diffuse transmission. Using this macroscopic detection for the Lévy exponent we found $\alpha = 2.1 \pm 0.1$, close to the value obtained with our microscopic protocol ($\alpha = 2.09$), validating the two different experimental schemes to measure Lévy flights of photons in atomic vapors. In our macroscopic detection scheme, we can also extract the Lévy exponent by analyzing the spatial profile of the transmitted light, adding a complementary observable to the study of anomalous diffusion of light.[46] The study of the spatial profile allows in particular to extract the Lévy exponent without requiring a systematic change of the opacity of the sample. This can become relevant for astrophysical systems, where it is not possible to change an experimental parameter to look for specific scaling laws. For astrophysical systems with opaque atmospheres, a comparison to our macroscopic detection scheme of Lévy flights might be possible (Fig. 9) and could be confirmed via numerical tests and specifically designed experimental geometries.

2.4. *Summary and outlook*

In this section we have shown that scattering of light in cold and hot atomic vapors allows the study of multiple scattering phenomena also expected to occur in astrophysical situations. We have in particular investigated the case of open atomic transitions and the role of Doppler broadening. These experiments illustrate the potential of modern tools in atomic, molecular and optical physics. Straightforward extension of these techniques include the study of the nature of the frequency redistribution (complete or partial frequency redistribution), the effect of collisional broadening (using buffer gas), the analysis of the Stokes parameters (relevant for instance in Faraday rotation experiments conducted in our group[23,48] but also used in astrophysics[49]). The use of larger intensities leading to the saturation of the Doppler-broadened transition is also in the range of today's lasers. Inelastic and/or nonlinear effects combined to Lévy flights will certainly create novel
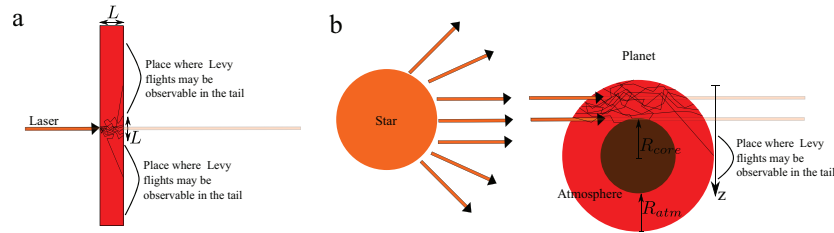
Cold and hot atomic vapors: a testbed for astrophysics?   17

Fig. 9. Analogy between our experiment[46] (a) and a possible astrophysics experiment(b). A planet with an opaque atmosphere (such as Venus) is illuminated by a star (for example the sun). The intensity distribution detected behind the planetary core might reveal the presence of Lévy flights for some frequencies resonantly scattered by atoms or molecules.

situations with yet unexpected features. Using our macroscopic protocol to detect Lévy flights, time-resolved experiments in the Lévy regime are also possible. It will be interesting to study whether in that case, the transport time will still be constant or whether one needs to consider a transition to a constant transport velocity. If the distribution of transport times has a power-law tail ("heavy tailed"), Lévy walks with super- as well as subdiffusive transport is possible.[32] In static samples (such as white paper or white paint) or in non resonant scattering samples with motion (such as milk) the fluctuations of transmission are also related to the spatial correlation function. To what extent such space-time fluctuations are affected by Lévy flights is still an open question and can now be addressed experimentally and theoretically. The interactions of light with hot and cold atomic vapors is obviously also of large interest for other communities, such as quantum information. We have seen that EIT might also appear in the multiple scattering regime and storage of quantum information in this limit will require a quantum optical approach.[50]

Despite all this potential and the fact that light scattering in stars and interstellar vapors requires a description in terms of Lévy flights, we acknowledge only limited direct interactions with researchers in astrophysics. Nevertheless, the direct comparison of our experimental results with numerical codes used in the measurement of the magnetic field on the surface of the sun has allowed for a correction of these codes. These codes, on the other side, include the complex Zeeman structure of atoms and we will compare the results of the measurement of the Stokes parameters in our experiment to predictions obtained by the group of Marianne Faurobert at the Observatoire de la Côte d'Azur in Nice. Preliminary discussions with

18   *Q. Baudouin, W. Guerin, and R. Kaiser*

experts in intensity correlations in astrophysics motivate us to also consider a more precise study of the photon statistics emerging from hot and cold atomic vapors in both the single scattering and the multiple scattering regime.

3. Gain, lasing, and random lasing in atomic vapors

As early as 1968, Letokhov investigated what happens when amplification of light, or *gain*, is present in a multiple scattering medium.[51] In such a situation, multiple scattering increases the length of the path of light propagating in the gain medium and thus enhances its amplification. This obvious effect can lead to a much less trivial phenomenon, which is that there is a threshold on the system size above which amplification in the medium overcomes leakage at the surface, leading to an exponential increase of the light intensity trapped in the medium (and the subsequent emitted light).[51,52] This is very similar to the principle of a laser, which starts when gain produced by the amplifying medium overcomes the cavity losses. Here, the cavity is replaced by radiation trapping, which provides an "incoherent" feedback. Since there is no cavity axis to impose a propagation direction, the emission diagram is more or less random (like a speckle pattern), hence the name random laser. Like in a standard laser, the exponential increase of the light intensity is limited by gain saturation to a value for which gain exactly compensates losses.

After some preliminary evidence of scattering-enhanced emission of light in some gain media,[53–55] great efforts have been made in the last 15 years to experimentally demonstrate and study random lasing in different kinds of systems.[56–60] It has immediately appeared that Letokhov's initial theory, which is based on the diffusion equation and thus neglects any interference effect, was not sufficient to describe random lasers, which exhibit subtle mode and coherence properties. The understanding of these properties is a theoretical challenge, as it is related to fundamental questions on the nature and properties of electromagnetic modes in open and/or disordered systems,[61–63] and different theoretical approaches have been developed.[64–70] The broad interest of random lasing is also driven by potential applications.[71] For instance, the use of a random laser as a light source for speckle-free laser imaging has been recently demonstrated.[72]

State-of-the-art random lasers are usually based on pulsed excitation of condensed matter systems and quasi cw operation of random lasing in dilute atomic vapors had not been realized prior to our recent study.[73]

Cold and hot atomic vapors: a testbed for astrophysics?   19

3.1. *Astrophysical lasers*

The subject of random lasers based on atomic and molecular gases has been introduced, by Letokhov himself, in the context of astrophysical lasers. Indeed, astronomical observations in the microwave domain have led to the discovery of anomalously bright emission lines from molecules in stellar atmospheres.[74] It was soon understood that the only possible explanation was an amplification of the corresponding wave due to stimulated emission.[75] The study of these astrophysical masers, which turned out to be very common, has been an important research subject in the 1970s.[76,77]

Emission lines with anomalous intensities were also known in the optical domain[78,79] without any convincing explanation. Letokhov suggested that they could also be explained by stimulated emission, and that scattering-induced feedback could enhanced the amplification, even reaching the oscillatory regime,[80,81] a phenomenon that would be called a random laser today.

Amplification by stimulated emission was indeed observed in the planetary atmospheres of Mars and Venus in the infrared (IR) domain ($\lambda \sim 10\,\mu$m)[82,83] and much later in stellar atmospheres in the far IR.[84] More recently, astrophysical lasers in the near IR was discovered by Johansson and Letokhov, based on Fe II[85] and O I.[86] In the optical domain, population inversion is much harder to obtain than in the microwave domain, and astrophysical lasers are very rare, contrary to masers.[87]

It should be noted here that astrophysicists often call "lasers" what a laser physicist would describe as amplification, or Amplified Spontaneous Emission (ASE).[3] The existence of additional feedback due to multiple scattering seems to be an open question. In the microwave domain, there are ununderstood bursts of radiation from the water vapor maser in Orion KL,[88] and scattering-induced feedback in the oscillatory regime (i.e., random lasing above threshold) has been proposed as a possible explanation.[89] The latest observations, however, do not seem to confirm this idea.[90]

Nevertheless, it seems that the ingredients necessary for a random laser, that is, multiple scattering and stimulated emission, are both present in stellar gases.[91] Laboratory experiments on random lasing in atomic vapors may help us better understand the precise necessary conditions for random lasing to occur in space. The study of the properties of the light emitted by atom-based random lasers could also help us design appropriate detection tools[92] to find signatures of scattering-induced feedback in astrophysical lasers.

20   *Q. Baudouin, W. Guerin, and R. Kaiser*

3.2. *Gain and lasing with cold atoms*

As discussed in Sec. 2.2, standard MOTs have on-resonance optical thickness on the order of $b_0 \sim 10-50$, which is largely enough to induce multiple scattering and radiation trapping.[19] In this section, we present how *gain*, the second ingredient of random lasers, can be obtained from a cold-atom cloud.

Contrary to most laser gain media, cold atoms do not present non-radiative, fast-decaying transitions, preventing a standard 4-level scheme to produce a population inversion. Nevertheless there are many different mechanisms which allow an inversion between two different atomic states. These can either be different states in external degrees of freedom (momentum or vibrational levels in an external potential) or internal degrees of freedom (dressed states[93] or different ground states). The atomic non-linearity can also be used to obtain parametric gain and lasing, as well as other, more complicated schemes using quantum interferences.

3.2.1. *Mollow gain*

A very simple gain mechanism in atomic vapors was described by Mollow[95] and observed soon afterwards[96] with atomic beams. It involves a two-level atom driven by one strong pumping field. The driving field induces a population inversion in the dressed-state basis[93] and therefore a weak probe beam can be amplified. The whole process can also be described

Fig. 10.   (a) Principle of the Mollow gain depicted as a three-photon transition from the ground state to the excited state, with two absorptions from the pump at ω_P and one stimulated emission in the signal wave at ω_S. It can also be viewed as a population inversion in the dressed-state basis. (b) Transmission spectrum, computed for typical experimental parameters $b_0 = 10$, $\Omega = 2\Gamma$ and $\Delta = \Gamma$. From.[94]

in the bare-state basis by a three-photon transition from the ground state to the excited state via two absorptions of pump photons as sketched in Fig. 10(a).

The main amplification feature appears for a pump-probe detuning of $\delta = \text{sign}(\Delta)\sqrt{\Delta^2 + \Omega^2}$, where Δ is the pump detuning from the atomic transition, Ω is the Rabi frequency of the pump-atom coupling, related to the pump intensity I by $\Omega^2 = \Gamma^2 I/(2I_{\text{sat}})$ (I_{sat} is the saturation intensity), and has a typical width on the order of the transition linewidth Γ. Note that another, dispersion-like feature appears around $\delta = 0$, which is associated with two-photon spontaneous emission processes.[97] This contribution also induces gain with a much smaller amplitude, and can generate lasing without population inversion.[98,99]

In our experiment with cold ^{85}Rb atoms, we have measured single-pass gain as high as 50 %, which is more than enough to induce lasing, even with a low-finesse cavity.[100] We have thus realized a Mollow laser with cold atoms with an output intensity reaching 35 μW achieved for $|\Delta| \sim 2\Gamma$. Its threshold in pump intensity is in agreement with the corresponding measured single-pass gain and the losses of the cavity. The polarization of the emitted laser is linear, parallel to the pump polarization, because this is the configuration for which gain is maximum, as the driven atomic dipole is then parallel to the probe field.

3.2.2. *Raman gain using Zeeman sublevels*

Another gain mechanism in atomic vapors is Raman gain. Raman transitions refer in general to two-photon transitions between two non-degenerate ground states, the intermediate energy level being in the vicinity of an atomic excited states. To obtain gain, a pumping field can induce the first upward transition and a probe beam can then be amplified at the frequency of the downward transition.

A first possibility is to use the pump-induced population inversion among the different light-shifted Zeeman sublevels m_F of a given hyperfine level F, as depicted in figure 11(a).[101,102] For example, optical pumping near a closed $F = 1 \rightarrow F' = 2$ transition induced by a π-polarized laser leads to a symmetric distribution of population with respect to the $m_F = 0$ sublevel of the ground state, with this sublevel being the most populated and also the most shifted, due to a larger Clebsch-Gordan coefficient.[103] To record a transmission spectrum, atoms are probed with a linearly polarized probe beam with the polarization axis orthogonal the pump polarization,
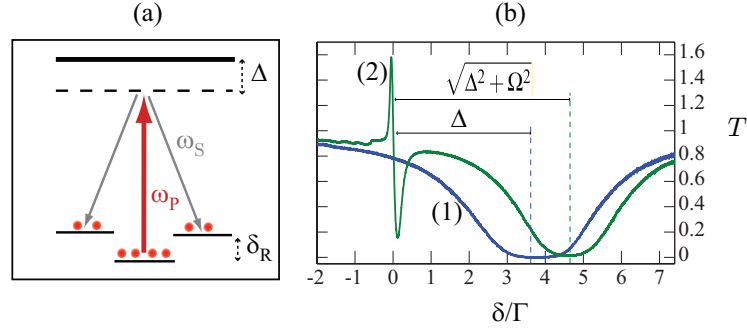
22   *Q. Baudouin, W. Guerin, and R. Kaiser*

Fig. 11.   (a) Principle of the Raman mechanism, depicted here for a $F = 1 \to F' = 2$
transition. (b) Experimental transmission spectra recorded with cold ^{85}Rb near the
$F = 3 \to F' = 4$ transition, plotted as a function of the pump-probe detuning δ.
Without pumping, spectrum (1) shows only the atomic absorption. A pump beam of
detuning $\Delta = -3.8\ \Gamma$ and intensity 13 mW/cm^2, corresponding to a Rabi frequency
$\Omega = 2.5\ \Gamma$, is added to obtain spectrum (2), which then exhibits a Raman resonance in
the vicinity of $\delta = 0$. Moreover, the atomic absorption is shifted due to the pump-induced
light shift and the absorption is reduced due to saturation. From.[94]

thus inducing $\Delta m_F = \pm 1$ Raman transitions. Depending on the sign of
the pump-probe detuning δ, the population imbalance induces gain or ab-
sorption. With a larger F, each pair of neighboring sublevels contributes
with a relative weight depending on the population inversion. In practice
however, the contributions of different pairs are often not resolved and only
two structures (with opposite signs) are visible, one corresponding to am-
plification for $\delta = -\delta_R$ and one to absorption for $\delta = \delta_R$. Note that this
situation corresponds to a red detuning for the pump ($\Delta < 0$) and that
the signs are inverted for blue-detuning ($\Delta > 0$). As δ_R comes from a dif-
ferential light-shift (because of different Clebsch-Gordan coefficients), it is
usually small, on the order of $\Gamma/10$, whereas Δ is a few Γ. The width γ of
the resonances is related to the elastic scattering rate, also much smaller
than Γ.[102]   Far from the main atomic absorption resonance, the Raman
resonance is thus a narrow spectral feature, as shown in Fig. 11(b).

   This mechanism has also been used to generate lasing with a MOT
inside an optical cavity.[100,104] The output polarization is orthogonal to the
pump one (contrary to the Mollow laser) and, in our experiment,[100] this
gain produces a laser with less power (2 μW). Moreover, the sharpness of
the gain curve makes the Raman gain very sensitive to any Doppler shift.
Thus, the radiation pressure from the pump beam makes the laser emission
stop after only $\sim 20\ \mu$s. On the other hand, the narrow spectrum of the

Cold and hot atomic vapors: a testbed for astrophysics?   23

laser can be easily characterized by a beat-note experiment.[100]

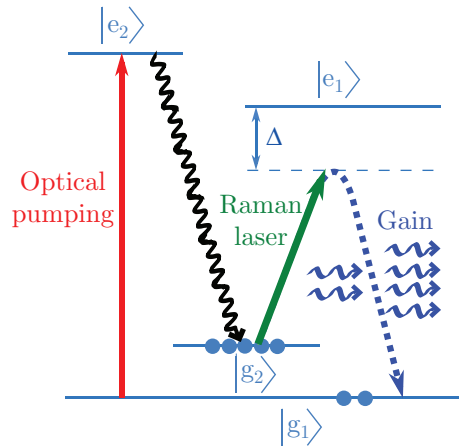### 3.2.3. *Raman gain using hyperfine levels*

Fig. 12.   Raman gain using hyperfine levels. Gain is produced by stimulated emission induced by the Raman laser (two-photon transition). The population inversion between the ground states $|g_1\rangle$ and $|g_2\rangle$ is sustained by the optical pumping laser. Adapted from.[73]

The two hyperfine ground states of rubidium atoms can also be used to produce Raman gain. One advantage is that the gain and the pump frequencies are separated by several gigahertz. A drawback is that the pump laser has to be tuned close to an open transition, so that optical pumping quickly destroys any population inversion. A second laser is thus necessary to recycle the atoms (Fig. 12), which somewhat complicates the setup.

This gain mechanism has been used in different beautiful experiments on lasing with cold atoms in different regimes[105–107] and our experiment on random lasing also uses this gain (see sections 3.3.4 and 3.4).

3.2.4. *Parametric gain: four wave mixing*

By using two phase-locked pump beams, we can induce four wave mixing (FWM): the two pumps of frequencies ω_{P1} and ω_{P2} and one probe – or an initial fluctuation – of frequency ω_S generate a fourth field at frequency ω_C, called the conjugate field.[108–110]   The frequencies and wave-vectors
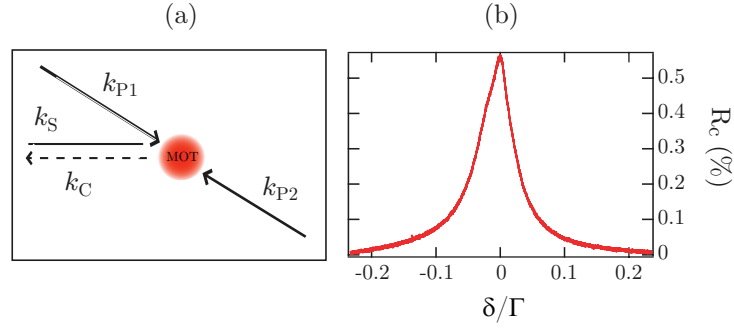
Q. Baudouin, W. Guerin, and R. Kaiser

Fig. 13.   (a) Principle of four-wave mixing. (b) Typical experimental reflection spectrum. From.[94]

of all the fields are related by energy and momentum conservation. If we want to obtain *gain* for the probe, we have to choose a configuration where the conjugate frequency equals the probe: $\omega_C = \omega_S$. Then, the pump frequencies have to fulfill the condition $\omega_{P1} + \omega_{P2} = 2\omega_S$. From an experimental point of view, the most simple configuration is when all frequencies are the same ("degenerate FWM"). This is the experimental situation with which lasing has been obtained, either with a cavity in our group,[100] or with distributed feedback (DFB) in Tübingen, using atoms trapped in a 1D optical lattice.[111] Note that this mechanism has been observed a long time ago with hot atoms.[112–114]

Due to the phase matching condition, gain is not in the forward transmission of the probe beam, but in backward reflection, provided that the two pumps are counterpropagating (Fig. 13). The conjugate beam is actually the phase-conjugate of the probe beam. This property has a number of consequences for the cavity-laser.[100] First, it leads to a different threshold condition:[113] a reflectivity of only 1 % is enough to generate lasing, despite the much larger losses of the cavity (in our experiment, 32 % for a round trip). This is due to constructive interferences between transmitted and reflected waves, as observed in double-pass experiments.[115] Second, it leads to more complex transverse modes, because the phase conjugation mechanism allows any transverse pattern to be stable through the resonator.[116] Finally, these properties lead to a much larger power than with Mollow and Raman gain, and up to 300 μW have been obtained. The phase-conjugation property is also important for the DFB laser of Tübingen, since it participates in the feedback to make it stable.[111,117]

Another configuration of parametric gain is possible, that is non-

degenerate FWM, for which two different frequencies ω_F and ω_B are used for the two pump fields, and amplification occurs at frequency $\omega = (\omega_F + \omega_F)/2$. This configuration seems *a priori* promising for random lasing, since it allows one to adjust the gain frequency close to the atomic frequency ω_0 to enhance scattering. We have experimentally characterized this parametric gain and obtained that, although a conjugate field can indeed be produced near the atomic resonance, it cannot overcome the losses due to inelastic scattering.[118] This configuration is thus not appropriate for random lasing.

3.2.5. *Other gain mechanisms*

The above list of the possible gain mechanisms that can be used in cold atoms is not exhaustive.

Other, more complicated, schemes involve quantum interferences to induce gain without population inversion (in any basis).[99] This can be realized with a Λ scheme[119] or a V scheme.[120,121]

Another possibility is to use the atomic external degrees of freedom, i.e., their kinetic energy. Transitions between different velocity classes produce recoil-induced resonances,[122] and high gain can be achieved.[123] These resonances can ultimately lead to a "Collective atomic recoil laser",[124,125] which has been demonstrated with cold and ultra-cold atoms.[126,127]

Finally, one could also consider higher-order photonic processes, such as two-photon dressed-state lasers.[128]

3.3. *Combining gain and scattering: threshold of a random laser in cold atoms*

The peculiarity of a random laser based on cold atoms is that the same microscopic elements (the atoms) should provide both ingredients (scattering and gain) of random lasing. On the one hand, it leads to an easier characterization and modeling of the microscopic properties of the system, which can be extremely valuable for a better understanding of the physics of random lasers. On the other hand, it is clear that pumping atoms to induce gain drastically reduces their scattering cross-section, due to the saturation effect:[93] atoms spend less time in their ground state, in which they can scatter light. Moreover, in almost all gain mechanisms presented in the previous section, gain is obtained in a very narrow range of frequency, detuned from the atomic transition, leading to a reduced scattering cross section at that frequency. It is thus not obvious at all that reasonable con-

26   *Q. Baudouin, W. Guerin, and R. Kaiser*

ditions for random lasing can be obtained in cold atoms. Moreover, these
conditions are expected to be different for each gain mechanism. To choose
the best one, it is thus necessary to devise a quantitative criterion on the
possibility of random lasing.

3.3.1. *Threshold of a random laser in the diffusive approximation*

Following Letokhov's approach to derive a threshold condition for cw op-
eration of random lasing,[51,52] we start from the diffusion equation for light
with a gain term,

$$\frac{\partial W(\mathbf{r},t)}{\partial t} = D\nabla^2 W(\mathbf{r},t) + \frac{v}{\ell_{\mathrm{g}}} W(\mathbf{r},t) \,, \tag{12}$$

where W is the energy density, v is the transport velocity inside the medium,
ℓ_{g} is the gain length and D is the diffusion coefficient given by Eq. (6).

Taking into account the finite size L of the medium and using as bound-
ary condition that $W(L+z_e,t) = 0$, where z_e is the extrapolation length,[16]
one can show, using a modal decomposition,[51,52] that the time dependence
of W changes from an exponential decrease to an exponential increase when
crossing the threshold

$$D\left(\frac{\beta\pi}{L_{\mathrm{eff}}}\right)^2 - \frac{v}{\ell_{\mathrm{g}}} = 0 \,, \tag{13}$$

where $L_{\mathrm{eff}} = L + z_e$ is the effective length of the medium and β is a numerical
factor that depends only on the geometry ($\beta = 1$ for a slab of thickness
L, $\beta = 2$ for a sphere of diameter L and $\beta = \sqrt{3}$ for a cube). Using the
expression of D (and taking from now on $\beta = 2$), the threshold can be
written as a critical sphere diameter

$$L_{\mathrm{eff}} > 2\pi\sqrt{\frac{\ell_{\mathrm{sc}}\,\ell_{\mathrm{g}}}{3}}. \tag{14}$$

We note $L_{\mathrm{eff}} = \eta L$, where $\eta \sim 1$ is a small correction in the diffusive regime.
For a sphere geometry, $\eta = 1 + 2\xi/\left[L/\ell_{\mathrm{sc}} + 2\xi\right]$ with $\xi \simeq 0.71$.[129,130] The
diffusive, or multiple-scattering regime, is reached when $L \gg \ell_{\mathrm{sc}}$, which
corresponds to the validity range of this threshold condition, which we will
call Letokhov's threshold.

3.3.2. *Threshold of a random laser using the radiative transfer equation*

In a regime of low scattering, transport of light can be described using the radiative transfer equation (RTE),[131] which is valid from the ballistic regime to the diffusive one.[132]

The basic quantity of the RTE is the specific intensity $I_\omega(\mathbf{r}, \mathbf{u}, t)$, which describes the number of photons at frequency ω, at point $\mathbf{r}$, propagating along direction $\mathbf{u}$ at time t. In the case of plane-wave illumination along the z direction, and for isotropic scatterers, the specific intensity only depends on the space variable z and the angular variable $\mu = \cos\theta$, with θ the angle between the propagation direction $\mathbf{u}$ and the z-axis. In a system exhibiting gain and (isotropic) scattering, the RTE reads

$$\frac{1}{v}\frac{\partial I_\omega}{\partial t}(z,\mu,t) + \mu\,\frac{\partial I_\omega}{\partial z}(z,\mu,t) = -(a+\chi)I_\omega(z,\mu,t)$$
$$+ \frac{\chi}{2}\int_{-1}^{+1} I_\omega(z,\mu',t)\,\mathrm{d}\mu'\,, \quad (15)$$

where v is the energy velocity in the medium, a is the linear absorption coefficient and $\chi = \ell_{\mathrm{sc}}^{-1}$. For a medium with gain, $a < 0$ and it is better to use the linear gain coefficient $g = -a = \ell_{\mathrm{g}}^{-1} > 0$.

In one dimension, the RTE has a modal expansion, whose asymptotic behavior at large length and time scales leads to the modal expansion of the diffusion equation.[129] Therefore, under the conditions of uniform (in space) and constant (in time) gain, it is possible to build a modal theory of random lasers with incoherent feedback based on the RTE, that generalizes Letokhov's theory beyond the diffusive regime,[94,133,134] extending the validity of the threshold condition to low scattering samples down to $L \sim \ell_{\mathrm{sc}}$.

For a spherical medium in three dimensions, to the best of our knowledge, no model expansion of the RTE is available. However, as shown by Letokhov *et al.*,[3,81,91] the RTE can directly be solved by using the so-called Eddington approximation.[135,136] One obtains a critical radius R_{cr} given by

$$\tan(qR_{\mathrm{cr}}) = \frac{2gqR_{\mathrm{cr}}}{2g - q^2 R_{\mathrm{cr}}}\,, \quad (16)$$

with

$$q^2 = 3g(\chi - g) = \frac{3}{\ell_{\mathrm{g}}}\left(\frac{1}{\ell_{\mathrm{sc}}} - \frac{1}{\ell_{\mathrm{g}}}\right)\,. \quad (17)$$

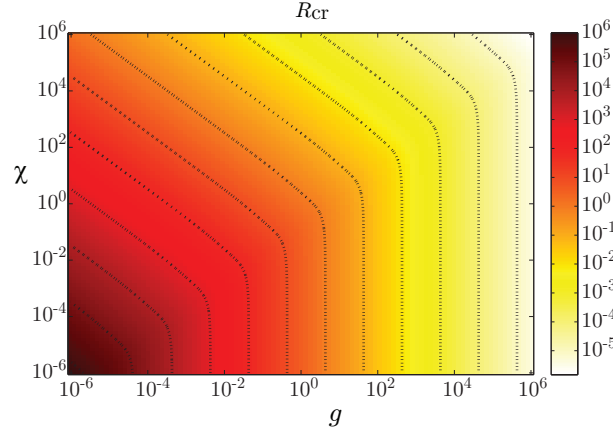28   *Q. Baudouin, W. Guerin, and R. Kaiser*

Fig. 14.   Numerical solution of Eq. 16. Note the log scales. The dotted lines are iso-R_{cr} contours. In the upper left part, the threshold condition is well described by a diffusion model, whereas in the lower right part, R_{cr} is independent on the scattering length, similar to ASE.

To recover the threshold given by Eq. (14) one needs to suppose that there is much more scattering than gain ($\chi \gg g$ so that $q^2 \simeq 3g\chi$) and also that $\chi R_{cr} \gg 1$ (diffusive regime). One can then easily show that the r.h.s. of Eq. (16) is very small. Then $qR_{cr} \sim \pi$, $L_{cr} \sim 2\pi/q = 2\pi(\ell_g \ell_{sc}/3)^{1/2}$.

Interestingly, one can also simplify Eq. (16) in the opposite limit of very low scattering and high gain. With the hypothesis $g \gg \chi$ and $gR_{cr} > 1$, we have the simplification $q \simeq \pm ig\sqrt{3}$ and $\tan(qR_{cr}) \simeq \pm i$, and Eq. (16) is easily solved to[b] $R_{cr} \sim 1/\left[\left(\sqrt{3} - 3/2\right)g\right] \approx 4/g$. Very surprisingly, the result is independent of χ, which suggests that a threshold exists even without scattering. This result might be due to a breakdown of the Eddington approximation in the limit of vanishing scattering.[137,138]

The numerical solution of Eq. (16) is shown in Fig. 14. It shows a smooth transition between the diffusive regime to a quasi-ballistic regime.

3.3.3.   *Application to cold atoms*

For an atomic vapor, the characteristic lengths entering the random laser threshold are both related to the atomic polarizability $\alpha(\omega)$ at frequency ω. The extinction cross-section is indeed given by $\sigma_{ex}(\omega) = k \times \text{Im}[\alpha(\omega)]$ and the elastic scattering cross-section by $\sigma_{sc}(\omega) = k^4/6\pi \times |\alpha(\omega)|^2$ ($k = \omega/c$ is the wave vector).[13] Note that the first relation is general to any

---

[b]Note that there is a misprint in Letokhov's papers.[3,81,91]

dielectric medium whereas the second one is specific to dipole scatterers. The characteristic lengths are then $\ell_{\mathrm{ex,sc}}^{-1} = \rho\,\sigma_{\mathrm{ex,sc}}$, where ρ is the atomic density. The gain cross-section can be defined the same way by $\ell_{\mathrm{g}}^{-1} = \rho\,\sigma_{\mathrm{g}}$, using $\ell_{\mathrm{ex}}^{-1} = \ell_{\mathrm{sc}}^{-1} - \ell_{\mathrm{g}}^{-1}$. Assuming that the density and pumping parameters are homogeneous, both ρ and α are position-independent. Even though this may be a strong approximation in some cases, it allows us to perform analytical estimations. As we consider resonant scatterers, we deal only with quasi-resonant light and we shall use $k = k_0 = \omega_0/c$ with ω_0 the atomic eigenfrequency. In the following, we shall also use a dimensionless atomic polarizability $\tilde{\alpha}$, defined as $\alpha = \tilde{\alpha} \times 6\pi/k_0^3$, and omit the dependence on ω. We can now rewrite $\sigma_{\mathrm{sc}} = \sigma_0 |\tilde{\alpha}|^2$ and $\sigma_{\mathrm{g}} = \sigma_0 \left[|\tilde{\alpha}|^2 - \mathrm{Im}(\tilde{\alpha}) \right]$, where $\sigma_0 = 6\pi/k_0^2$ is the resonant scattering cross-section (for a $J = 0 \to J = 1$ transition), such that the threshold condition, as given by Eq. (14), reduces to[134]

$$\rho\sigma_0 L_{\mathrm{eff}} = \eta b_0 > \frac{2\pi}{\sqrt{3|\tilde{\alpha}|^2 \left[|\tilde{\alpha}|^2 - \mathrm{Im}(\tilde{\alpha}) \right]}}\,, \tag{18}$$

where $b_0 = \rho\sigma_0 L$ is the on-resonance optical thickness of the cloud. This condition is valid in the diffusive regime as soon as the medium exhibits gain, i.e., $|\tilde{\alpha}|^2 - \mathrm{Im}(\tilde{\alpha}) > 0$. Interestingly, the condition $\mathrm{Im}(\tilde{\alpha}) < 0$, corresponding to single-pass amplification (transmission $T > 1$), is not a necessary condition.

The threshold condition is thus given by a critical on-resonance optical thickness, which is an intrinsic parameter of the cloud, expressed as a function of the complex atomic polarizability only, which depends on the pumping parameters. Although the initial condition of Eq. (14) involves two characteristic lengths, we emphasize here that this is really one single physical quantity, as real and imaginary parts of the atomic polarizability are related via Kramers-Kronig relations.[139] This point is due to the originality of the system that we are considering, in which the same atoms are used to amplify and scatter light. This property can be fruitfully used to experimentally determine the threshold, as only one single measurement can provide enough information. A weak probe transmission spectrum, which we can rewrite with our notations,

$$T(\omega) = e^{-b_0 \,\mathrm{Im}[\tilde{\alpha}(\omega)]}\,, \tag{19}$$

indeed allows the full characterization of $\tilde{\alpha}(\omega)$.[140]

30   *Q. Baudouin, W. Guerin, and R. Kaiser*

3.3.4. *Comparison between different gain mechanisms*

Using Letokhov's threshold given by Eq. (18), we can compare different gain mechanisms.[94,118] The atomic polarizability (or equivalently the cross sections) can be computed, sometimes analytically (for Mollow gain), more often numerically by solving the optical Bloch equations (OBEs), or they can be determined experimentally from transmission spectra, as explained above.

For Mollow gain, we can use an analytical expression of the polarizability,[95] which depends on two pumping parameters, the atom-pump detuning Δ and the pump intensity parameterized by the Rabi frequency Ω. For each couple of pump parameters, one can search for the frequency of the emitted light leading to the lowest critical b_0, since the random laser will start lasing at the optimum frequency. This procedure allowed us to determine the threshold for this gain and we obtained[134] $b_{0\mathrm{cr}} \sim 200$.

For Raman gain between Zeeman sublevels, we have used measurement of transmission spectra to evaluate the atomic polarizability entering into Eq. (18) to determine the threshold.[140] We obtained a similar threshold $b_{0\mathrm{cr}} \sim 200$.

Raman gain between hyperfine ground states is more complicated to study, as it involves more pumping parameters. Indeed, to sustain a continuous gain, a Raman laser is needed to induce the Raman two-photon transition and an optical-pumping laser is needed to maintain the population inversion (see §3.2.3). There are thus two laser detunings and two laser intensities. Intuitively, one can expect that having more optimization parameters is favorable and should lead to a lower threshold. This is indeed what we obtain by numerically solving the OBEs and searching for the optimum parameters.[118] Fig. 15(a) shows the critical optical thickness as a function of the detuning and intensity of the Raman laser for optical pumping parameters that has been chosen to give the lowest minimum critical optical thickness, which is $b_{0\mathrm{cr}} \sim 100$. This is a substantial improvement in comparison with Mollow gain and Raman gain using Zeeman sublevels.

However, in all these scheme, the gain frequency is detuned by several atomic linewidths Γ from the atomic transition that provides scattering. As a consequence, the found optimum parameters correspond to a regime of low scattering, compensated by a high gain. On the one hand, this is interesting because it is quite different from all other kinds of random lasers. On the other hand, the diffusive approach is not valid any more, and one should use instead the RTE to compute the threshold. We have verified

Cold and hot atomic vapors: a testbed for astrophysics?   31

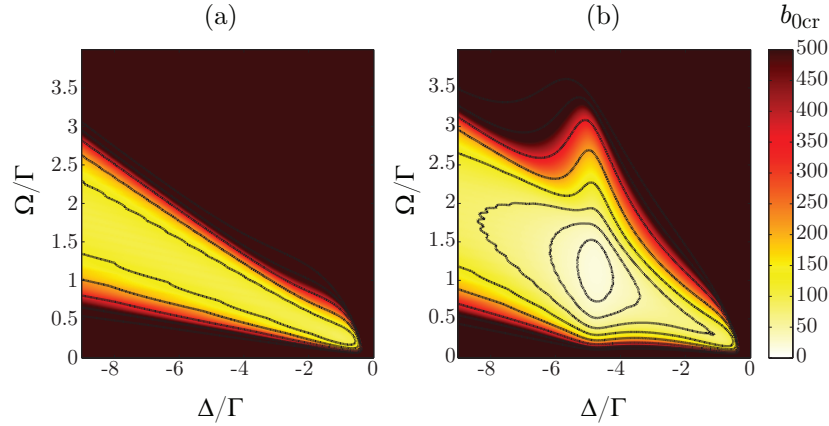that in 1D, it leads to very similar results.[134]

Fig. 15.   Threshold for a random laser using Raman gain between hyperfine levels, as a function of the Raman laser parameters (detuning Δ, Rabi frequency Ω). The optical pumping parameters are $\Delta_{\mathrm{OP}} = 0$ and $\Omega_{\mathrm{OP}} = 0.2\Gamma$. (a) Scheme with four levels. The lowest threshold is $b_{0\mathrm{cr}} = 92$. (b) Scheme with five levels involving supplementary scattering from the $|2\rangle \rightarrow |1'\rangle$ transition (Fig. 16). The lowest threshold is $b_{0\mathrm{cr}} = 20$. The contours are iso-$b_{0\mathrm{cr}}$ lines.

Raman gain with supplementary scattering   Fortunately, the rich atomic structure of the D_2 line of rubidium atoms (and other alkali metals) allows us to combine Raman gain between hyperfine levels with supplementary scattering provided by a closed transition. The scheme, represented in Fig. 16, involves five levels. As previously, two ground states ($|F = 2\rangle$ and $|F = 3\rangle$ in ^{85}Rb, noted from now on $|2\rangle$ and $|3\rangle$) and one excited states are necessary to build Raman gain in a Λ scheme (we use $|F' = 2\rangle \equiv |2'\rangle$), and one another excited level is used for optical pumping ($|F' = 3\rangle \equiv |3'\rangle$) to sustain the population inversion. In addition, another level ($|F' = 1\rangle \equiv |1'\rangle$) can provide scattering on the gain transition if the detuning Δ of the Raman laser from the excited $|2'\rangle$ level is chosen to be equal to the frequency separation between the $|1'\rangle$ and $|2'\rangle$ levels. This supplementary level has several important features. Firstly, it is not coupled to the ground state $|3\rangle$ by any dipole-allowed transition, so that it does not interact with the Raman laser and does not destroy Raman gain. Secondly, the transition $|2\rangle \rightarrow |1'\rangle$ is closed so that it is efficient for scattering and does not change the equilibrium populations in the ground states. Finally, the separation
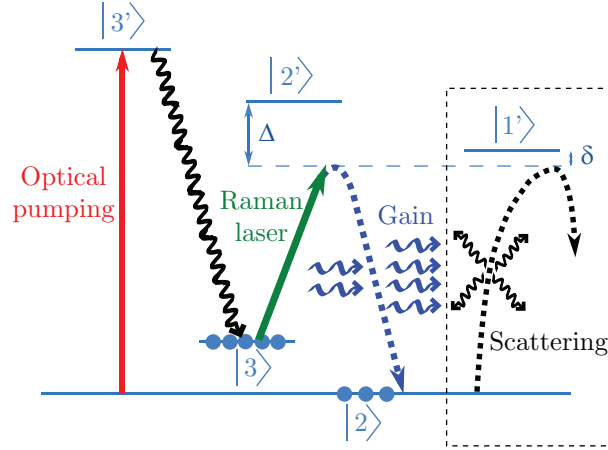
Fig. 16.   Scheme of the Raman gain used for random lasing in cold ^{85}Rb. Supplementary scattering is provided by the $|2\rangle \to |1'\rangle$ transition (dashed box). Adapted from.[73]

between the $|1'\rangle$ and $|2'\rangle$ levels is only 29 MHz, which is 4.8Γ. The necessary detuning Δ is thus small enough to insure that Raman gain is efficient. Note that a similar five-level scheme is possible by using the $|F' = 4\rangle$ level for supplementary scattering but its separation from the nearest level is 20Γ and Raman gain would be much less efficient (similarly, ^{85}Rb is more favorable than ^{87}Rb because hyperfine splittings are smaller).

The relative intensity between the two external lasers allows us to adjust the relative populations, and thus to tune continuously from a sample with large gain and no scattering (with all atoms in the $|3\rangle$ state) to a situation without gain and with large scattering on the $|2\rangle \to |1'\rangle$ line (with all atoms in the $|2\rangle$ state). We can therefore search for the best trade-off between gain and scattering. With the optimum parameters, we find a critical optical thickness of $b_{0\mathrm{cr}} \sim 20$ (Fig. 15(b)) with $L/\ell_{\mathrm{sc}} \sim 6$ at the threshold, so that the diffusion approximation is justified. The model is based on the OBEs with a supplementary incoherent scattering term due to the $|2\rangle \to |1'\rangle$ transition.[73,118] Note that our model neglects the Zeeman degeneracy and thus cannot use the correct relative weight of the different lines. It is thus not precise enough for quantitative predictions.

3.4. *Experimental evidence of random lasing*

We have implemented the five-level Raman gain scheme described above.[73] The experimental procedure is as follows. We prepare a sample of cold

atoms of ^{85}Rb with a magneto-optical trap. A controlled compression period provides a variable optical thickness b_0 with a constant number of trapped atoms. We then switch off all lasers and magnetic field gradients during 1 ms before applying strong counterpropagating Raman beams. The optical-pumping laser is tuned slightly below the $|2\rangle \to |3'\rangle$ transition. Note that with the chosen detunings, the external lasers operate in the single scattering regime. The Raman laser detuning is swept slowly around $\delta = 0$, where Raman gain is on resonance with the $|2\rangle \to |1'\rangle$ transition. We measure the total emitted fluorescence, which we collect with a solid angle of 10^{-2} sr, and we average the detected signal over ~ 4000 cycles. We repeat the measurement for different optical thickness while keeping the atom number constant. Variations in the fluorescence can thus only be related to collective features. Our observations are reported in Fig. 17.

Before commenting on the observations, it is important to precisely understand what we look at and why. We measure the *total emitted light* by the atomic cloud when the two external lasers are applied. This signal contains the random-laser light, but also light which is scattered from the two external lasers (and might be subsequently amplified for Raman-scattered light from the Raman laser). The separation between the different lines is indeed experimentally very difficult because they all are at the same wavelength $\lambda = 780.24$ nm and differ only from a few megahertz or gigahertz. Moreover, in random lasers, there is not any privileged emission direction that allows one to spatially separate the random-laser light. In usual random lasers, the separation is done either spectrally or temporally (using very short pump pulses), which is very important because the light scattered from the pump is much more intense than the random laser itself. In our system, however, the $|2\rangle \to |1'\rangle$ transition does not scatter light from the two external lasers. The random-laser line has thus a strength comparable to the one of the other involved transitions and that is why it is possible to detect the random laser signal in the total fluorescence. It should also be stressed that in a standard laser, the beam is well separated from the fluorescence of the gain medium, thanks to the cavity. This is not the case in our system, where both are measured together. Finally, it may be useful to have in mind that looking at the total emitted light is equivalent, due to energy conservation, to looking at the pump depletion (here the two external lasers).

A first signature of a collective behavior can be seen in a regime of negligible scattering, far from the $|2\rangle \to |1'\rangle$ transition (regions 1 of Fig. 17): amplified spontaneous emission (ASE) induces an overall increase of the

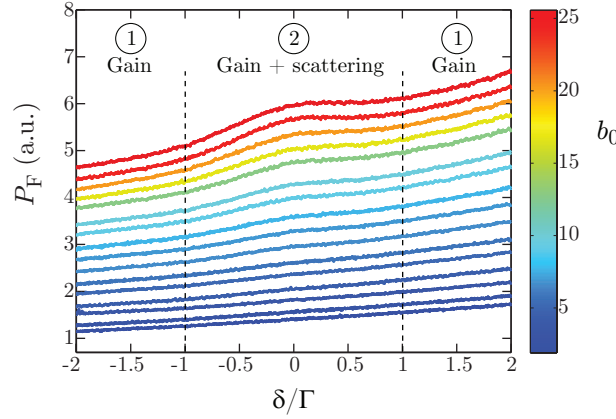34   *Q. Baudouin, W. Guerin, and R. Kaiser*

Fig. 17.   Measurement of the total fluorescence emitted by the cloud as a function of the Raman laser detuning for different on-resonance optical thickness b_0. Adapted from.[73]

fluorescence as a function of b_0. Photons from the Raman beam can indeed undergo a spontaneous Raman transition. The subsequent scattered light is then amplified by Raman gain produced by the surrounding atoms while leaving the sample with a ballistic path. The efficiency of this process is directly related to the optical thickness. The ASE signal decreases as the Raman laser is detuned further away from the $|3\rangle \rightarrow |2'\rangle$ transition (located at $\delta = +4.8\Gamma$) since both the spontaneous (source contribution) and stimulated (gain contribution) Raman scattering rates decrease for larger detuning. Note that when tuning the Raman laser very close to the $|3\rangle \rightarrow |2'\rangle$ line, single-photon scattering dominates. Population redistribution is then responsible for the increase of fluorescence[28] (see sec. 2.2.3 and Fig. 3). This effect is negligible for the detunings considered here, and only gain can explain the observed features.

When the Raman laser is tuned close to $\delta = 0$ (region 2 of Fig. 17), the combination of gain and scattering gives rise to an enhanced fluorescence bump that emerges as the optical thickness b_0 is increased. This feature is due to the combined effect of gain and scattering: multiple scattering increases the path length of the photons that are amplified by Raman gain. This is exactly the mechanism at the heart of random lasing. The only remaining question to be answered before concluding that we observe random lasing is to know if the system is above the threshold or not.

To answer this question, we plot the supplementary fluorescence as a function of the on-resonance optical thickness b_0. To better extract this

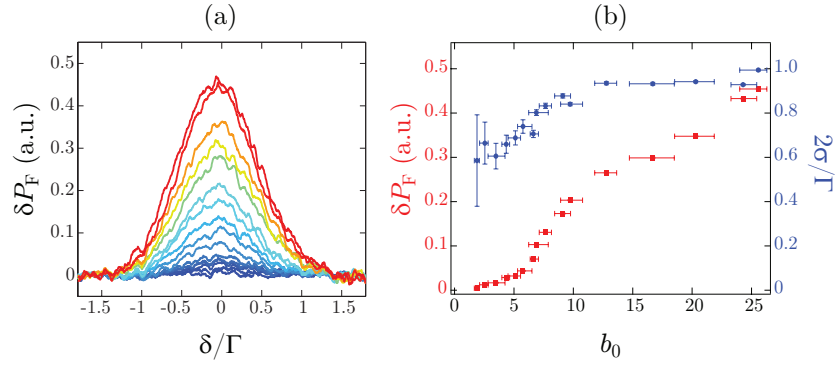*Cold and hot atomic vapors: a testbed for astrophysics?*   35

Fig. 18.   (a) Supplementary fluorescence around $\delta = 0$ for different optical thickness (same color scale as in Fig. 17). The raw data are the same as in Fig. 17 but the wings have been subtracted and the signal has been smoothed. (b) From a gaussian fit we extract the amplitude (red squares) and the r.m.s. width σ (blue circles) of the curves shown in (a) as a function of the optical thickness b_0. The vertical error bars are the statistical uncertainties of the fit (not visible for the amplitude) and the horizontal error bars correspond to the fluctuations of b_0 on 5 shots.

signal, we fit the wings of the curve (regions 1) by adjustable slope and curvature and remove this background. The remaining signal is a bell-shaped curve, well-centered at $\delta = 0$ (Fig. 18(a)). Surprisingly, it is very well fitted by a gaussian. We can thus use a gaussian fit to extract its amplitude and width, as reported in Fig. 18(b). Although the signal consists of different emission lines, a threshold of the peak amplitude is clearly visible, with a change of slope at $b_0 = 6 \pm 1$. We interpret this threshold as the signature of the occurrence of random lasing in our sample when the Raman beams are tuned around $\delta \sim 0$ and when $b_0 > 6$. We stress that varying the optical thickness acts simultaneously on the amount of gain and feedback provided by the medium. This is unusual in laser physics, where the threshold is most-commonly defined as a critical pump power. In our case, increasing the optical-pumping intensity increases indeed the population inversion that provides gain, but simultaneously decreases the feedback, so that random lasing needs a fine tuning of the laser parameters.

Our observations are in qualitative agreement with an *ab initio* model based on Letokhov's threshold.[73] There are however quantitative discrepancies. In particular, the measured threshold is lower than the predicted one. This may be due to interference and/or cooperative effects,[70] which are neglected in the diffusion model. Several other ingredients are neglected and might also play a role, like light polarization, the Zeeman degeneracy of

the involved atomic levels, the finite temperature of the cloud, and the inhomogeneous density distribution. This demonstrates the need for a more evolved modeling. Several theoretical approaches to random lasing have been developed in the last years[64–70] and the advantage of our experiment is to provide disorder-averaged data with perfectly known microscopic ingredients (rubidium atoms driven by two lasers with known frequencies and intensities), without any free parameters.

3.5. *Summary and outlook*

To summarize this part, we have shown that laser-cooled vapors are suitable media to provide gain and sustain lasing.[100] We have then investigated the possibility of combining gain and scattering to produce a random laser.[94,118,134,140] Finally, we have implemented an original configuration of Raman gain with supplementary scattering provided by an independent closed transition. This scheme has recently allowed us to demonstrate random lasing with cold atoms.[73]

Further work is needed for a more complete characterization of the system. An experimental challenge, in particular, consists in obtaining more direct observations of the random laser emission or of the transition at threshold. One possibility would be to spectrally filter the random laser line with a low-finesse Fabry-Perot cavity and study the statistical properties of the detected light. These efforts might help in designing detection methods that could also be appropriate for studying astrophysical lasers.

Our experiment has also to be compared in more detail with theory. The comparison between different models, each one including some, but not all, possible physical ingredients, should allow one to pinpoint which ingredients are relevant to random lasers in general and to random lasers based on atomic vapors in particular. This should be very useful for a better understanding of astrophysical lasers, especially the possible role of feedback induced by multiple scattering.

An ingredient that is certainly present in astrophysical lasers and that is not in a cold-atom random laser is the Doppler effect. One can wonder if random lasing is possible using a room-temperature vapor. Doppler broadening strongly reduces the efficiency of atom-light interaction (scattering and gain). It also induces a frequency redistribution that might be detrimental. However, an advantage is that it is easy, by heating a vapor cell, to reach very large optical thickness. A possibility would be to use a mixture of two isotopes, one for producing gain and the other for scatter-

Cold and hot atomic vapors: a testbed for astrophysics?   37

ing. Raman gain between hyperfine levels in hot vapors has already been used to demonstrate lasing.[141] By using the appropriate detuning, the gain provided by one isotope can be tuned to the scattering resonance of the other isotope. The investigation of this system will be the subject of future work.

4. Light-induced long-range forces

In astrophysics, it has been known for a long time that equilibrium properties of self-gravitating systems are rather special: negative specific heat, canonical (fixed temperature) and microcanonical (fixed energy) ensembles are not equivalent.[142,143] These anomalous features of long-range interacting systems have been fully appreciated by other physicists' communities only later. When long-range forces are considered, local properties of the particles in the cloud depend on all particles and thus on the total size of the system. Understanding the self-organizing behavior or the thermodynamics and out-of-equilibrium dynamics of long-range interacting systems is still a challenging objective. In d dimensions an isotropic interaction potential with $1/r^k$ yields a diverging mean field when $k < d$. This is for instance the situation of gravity in 3 dimensions and leads to the so-called Jeans instability, responsible for the formation of large scale structures such as galaxies.[144] In recent years it has been shown that statistical physics of long-range interacting systems generally exhibit a whole set of new qualitative properties and behaviors: temperature jumps, long-time relaxation (quasi-stationary states), violations of ergodicity, subtleties in the particle ("granular") picture, new macroscopic quantum effects, etc.[145] In contrast to the conservative regime, long range interacting systems with linear friction and white noise forcing have been studied in different contexts. Vlasov dynamics is then replaced by the Vlasov-Fokker-Planck equation, but quasi-stationary states are expected to survive.

These aspects are of course crucial in gravitational and Coulomb systems, but experiments with such long-range interactions are difficult to construct in a controlled way. Trapped cold atoms or ions are very interesting examples of mesoscopic systems, due to the possibility of manipulating their size and dimensionality through the trapping potential. As recognized by C. Wieman, multiple scattering of photons in cold atomic samples gives rise to a Coulomb-type long-range force scaling as $1/r^2$. MOTs thus share common features with one-component plasmas, even though important and qualitative differences exist. Cold-atom systems can thus exhibit

Q. Baudouin, W. Guerin, and R. Kaiser

non-extensive properties typical of long-range interactions. These interactions can either be dissipative or depend on the induced light shifts, similar to what has been studied in the context of optical binding.[146,147] Such forces would then become Hamiltonian and might find their application in coherent manipulation of atom-atom interactions. A number of theoretical proposals have been published using light induced forces, but their implementation on cold atomic samples is mainly limited to atoms in optical cavities,[148] as this enhances the light-induced coupling between the atoms, or in reduced geometries using atoms close to optical fibers.[149] The study of strongly correlated systems is another interesting feature because they can no longer be described by a mean field theory. In cold atoms, strong correlations of course appear if a modulated external potential is applied. This is an essential feature of optical lattices,[150] used, e.g., to create the Mott insulator in a Bose-Einstein condensate (BEC).[151] If long-range interactions can be engineered and applied to degenerate gases in a lattice, one could hope to see new exotic phases such as supersolids, where interactions between atoms further away than the next lattice site are required.[152]

The experiments conducted in our group in Nice aim at the understanding and experimental exploration of such long-range interactions. In this section, we will describe some of the systematic studies performed in the past and present and some predictions that will be considered for experimental exploration in the future.

4.1. *Scaling laws for MOT sizes*

Since the beginning of the manipulation of the position and the momentum of atoms by laser-induced forces, the achieving of high densities combined with low temperatures has been in the mind of many groups, with the goal of reaching the grail of Bose-Einstein condensation (BEC). Even though BEC is nowadays routinely achieved with different cooling techniques based on evaporation, it is interesting to recall the expectation that laser cooling of atoms seemed to offer. A Doppler model of MOTs has been used in the early days of laser cooling and trapping of neutral atoms, with a friction coefficient γ and a spring constant κ leading to a description of atoms in a MOT as a damped harmonic oscillator.[2] In that limit, the spatial extend of the atomic cloud is determined by its temperature and adding more and more atoms thus corresponds to a density increasing linearly with the atom number. As the critical temperature for BEC is given by $T_{cr} = (n/\zeta(3/2))^{2/3}(h^2/(2\pi m k_B))$, and with temperature in the range of $100\mu K$,

achieving BEC with, e.g., rubidium atoms ($m = 87 \times 1.67 \times 10^{-25}$kg) still required extremely high densities, of the order of $n = 10^{17}$ cm^{-3}. As one expected many difficulties, e.g., molecules formation, at such high densities, this lead many groups to focus on novel techniques to reach lower temperatures. Nevertheless, the quest for larger densities was important.

When a larger number of atoms are trapped in a MOT, it was recognized very quickly that the single atom description of laser cooling and trapping would not be reliable. Indeed, one initial estimate on the effect of collective feature of trapping many atoms has been based on the so-called shadow effect: if too many atoms are in the cloud, then the laser beams at the origin of the damping and spring constant will become attenuated during its propagation. If only this attenuation would be relevant, increasing the number of atoms would at a certain point leading to an increase of the confining forces of the MOT and the spatial density of atoms in the center of the cloud would increase faster than the total atom number.[153] It is interesting to note that similar arguments had been put forward by Le Sage in the 18$^{\text{th}}$ century to provide a model for gravitational attraction between two massive objects, even though this model is no longer considered today.[154] Even if this shadow effect does indeed play a role in the size of MOTs with large number of atoms, the photons which are screened by atoms at the boundary of the cloud also contribute with a net repulsion force when rescattered by other atoms. Due to the narrow resonance and the saturation of the atomic transition, the repulsion effect typically overcomes the attractive force in most MOTs. As recognized in,[155] the repulsion effect has the same binary interaction scaling as the Coulomb repulsion between charges of the same sign. One can then show that the maximum density of atoms in a MOT is limited to the "Wieman" limit:

$$n_{\text{W}} = \frac{\kappa}{G_3} \sim \frac{\kappa c}{2I_\infty \sigma_L(\langle \sigma_{\text{R}} \rangle - \sigma_{\text{L}})}. \qquad (20)$$

Here G_3 takes into account the balance between the shadow effect (scaling as the square of the scattering cross-section σ_L of photons at the incident frequency) and the repulsion by the rescattered photons (depending also on the average cross section $< \sigma_{\text{R}} >$ of scattered photons, some of them not at the same frequency as the incident photons), which in some limiting regimes can be approximated by an analytical expression.[156] Following this model, once the atom number is large enough, the spatial density is limited and the spatial profile of the atomic cloud is flat, as in a one component plasma in a harmonic trap. Experiments have indeed confirmed the limitation of the atomic density when the atom number exceeds typically 10^6, even though a

Q. Baudouin, W. Guerin, and R. Kaiser

quantitative comparison to the Wieman limit has not been successful.[157] It has also been noted that due to the Zeeman shift of the atomic transitions, the effective local detuning experienced by the atoms changes as a function of the distance of the atoms to the center of the cloud. At some distance this local Zeeman shift can overcome the detuning of the incident laser frequency and atoms will no longer experience an effective "red" detuned laser. This effect leads to a limitation of the maximum number of atoms which can be trapped with large laser beams.[158] The saturation of the atomic density due to multiple scattering has been an important limitation to the achievement of BEC with only optical laser cooling techniques. Multiple scattering of photons by cold atoms has thus been considered as a limiting phenomenon, which needs to be canceled in order to achieve BEC. One possibility is to "hide" the atoms in a dark hyperfine level. This technique, now often called dark MOT, initially demonstrated by W. Ketterle *et al.*,[159] is now used in most cold-atom experiments as it allows one to increase the spatial and/or optical density of cold-atom clouds to the "Wieman-Pritchard" limit

$$n_{\mathrm{WP}} = \frac{n_{\mathrm{W}}}{p},\qquad(21)$$

where p is the fraction of atoms in the hyperfine level interacting with the cooling and trapping lasers, which can be adjusted to some extend by a proper choice of the repumping laser parameters.

The limitations of dark-MOT techniques depend on various parameters, one of them being the temperature, as atoms hidden in the dark state can move out of the laser beams. Note that as MOTs with alkali atoms require a separate repump laser, the shadow effect and rescattering of the photons by this repump laser could also lead to limitations of the MOT density. In,[158] we have proposed a model that generalizes the Wieman-Pritchard model to include the rescattering of repump photons, giving

$$n_{\mathrm{WP+}} = \frac{n_{\mathrm{WP}}}{1 + \alpha \frac{I_{\mathrm{rep}}}{I_N} \frac{(1-p)^2}{p^2}},\qquad(22)$$

where α describes the ratio between the interaction of atoms in the bright and the dark hyperfine level, at a reference intensity for the repumper of I_N.

4.2. *MOT instabilities*

Beyond the study of MOTs in steady state, MOTs have been used to study a variety of instabilities. Exploiting the dependence of the cooling and trap-

Cold and hot atomic vapors: a testbed for astrophysics?   41

ping on the detuning of the laser beams, parametrically driven magneto-optical traps have been studied in.[160–162] These studies have allowed one to separate the Doppler and sub-Doppler components of the MOTs (with different dependance on the laser detunings) and spontaneous symmetry breaking of populations.[163] In the absence of any external modulation of control parameters, instabilities have been observed in different experiments. In the group in Lille, stochastic and deterministic instabilities have been studied.[164–166] The nonlinear equations used to explain the observed features are based on the attenuation of the laser beams, which for three retroreflected laser beams lead to important shadow effects with subsequent large displacements of the center of mass of the cloud. Note that whereas this shadow effect is usually not the dominant effect in a three dimensional MOT using independent laser beams,[153,155] it has been investigated for the possibility of long-range attraction in one dimension.[167]

In our group in Nice, we have studied instabilities in the size of the MOT using a six-beam configuration.[168–170] In this situation, an attenuation of the laser beams does not lead to a force along a bisectrix of the incident directions of propagation. The main ingredient at the origin of the instabilities reported in[168] is the repulsion force due to multiple scattering of photons in large clouds of cold atoms. This repulsion leads to an increase of the size of the cloud into the region where the local effective detuning is changing from negative ("red") detuning (with a friction allowing laser cooling) to positive detuning, where negative friction leads to an expulsion force of atoms beyond that horizon. One experimental signature of this self-sustained oscillation is the detected fluorescence signal shown in Fig. 19.

In contrast to the retroreflected instability, where the shadow effect pushes the center of mass of the cloud towards region where atom losses become important, we have verified that in our six-beam configuration, the observed instability does not rely on a loss of atom number. To explain these self-induced oscillations, we have used a simple model, based on a Doppler model of a MOT, with the main ingredient being the effective detuning experienced by atoms depending on their velocity (via the Doppler shift) and their position (via the Zeeman shift).[168] Assuming the total force acting on atoms to be given by

$$\boldsymbol{F}(\boldsymbol{r}, \boldsymbol{v}) = \boldsymbol{F}_{\mathrm{ms}}(\boldsymbol{r}) + \boldsymbol{F}_{\mathrm{MOT}}(\boldsymbol{r}, \boldsymbol{v}), \qquad (23)$$

where $\boldsymbol{F}_{\mathrm{ms}}(\boldsymbol{r})$ is the repulsion force induced by multiple scattering and $\boldsymbol{F}_{\mathrm{MOT}}(\boldsymbol{r}, \boldsymbol{v})$ describes the Doppler cooling and trapping of atoms in a MOT,

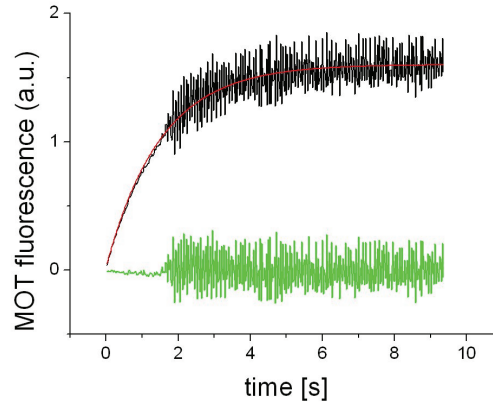42   *Q. Baudouin, W. Guerin, and R. Kaiser*

Fig. 19.   Self-induced oscillation of a MOT after switching on the MOT. A clear transition to oscillatory behavior is observed after some loading time, corresponding to a MOT size exceeding the critical size for stability (black line). After subtraction of an exponential function (red line), the increase of the oscillatory part is shown in green, consistent with a supercritical Hopf bifurcation.

one can see that the local friction coefficient $\gamma(\boldsymbol{r}) = \partial \boldsymbol{F}(\boldsymbol{r}, \boldsymbol{v})/\partial \boldsymbol{v}$ can change sign when the position of the atom located at the edge of the cloud is too large. Indeed, atoms located away from the center are subject to important Zeeman shifts, which reduce the effective detuning, leading to a spatially-dependent friction coefficient.

Analyzing the force experienced by a test atom located at the edge of the cloud and performing a linear stability analysis, we have derived a very simple equation for the threshold of instabilities,

$$\delta + \mu R \sim 0, \tag{24}$$

where μR is the Zeeman shift of the test atom located at a distance R from the center of the cloud and δ is the detuning of the MOT beams. This model also provides a qualitative classification of the observed instability, which we identified as a supercritical Hopf bifurcation. Qualitative experimental results confirm this classification : we have seen no indication of hysteresis (Fig. 20), the amplitude of the oscillation increases continuously from zero to some finite value (Fig. 19), whereas the frequency of the oscillation is nonzero at the onset of the oscillation.

This simple model is obviously neglecting many important details of the laser-atom interaction. It has however the advantage to identify a simple qualitative feature of the experimental observation. The mechanism of the

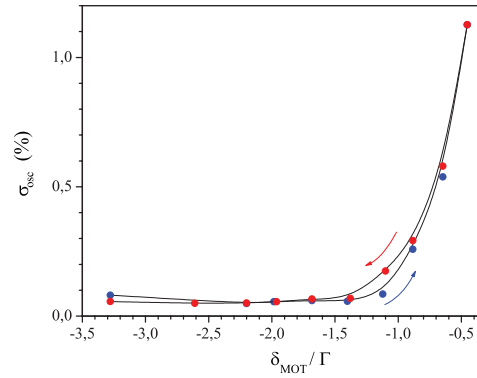*Cold and hot atomic vapors: a testbed for astrophysics?*   43

Fig. 20.   Amplitude of the measured oscillations as a function of the detuning of the MOT beams. Slow (0.1 Hz) forward and backward scans of the detuning show no hysteresis, indicating a supercritical Hopf bifurcation (from[170]).

instability lies in the negative friction of the edges of the atom cloud. In order to validate this simple model, we have performed a kinetic description of a large cloud of cold atoms. We have used an efficient test-particle method, taking into account the single-atom light pressure forces and including laser attenuation (shadow effect) and forces due to multiply-scattered light. Assuming a radial symmetry of the cloud to be maintained during all thr evolution we kept a position-dependent absorption cross sections (via the local Zeeman shift and intensities). One important result from this more evolved model is the confirmation of the qualitative estimation of the scaling law for the threshold condition. Furthermore this model allowed us to predict novel features, not observed so far in the experiment, such as shock waves entering into the center of the cloud or spatio-temporal structures[169] (Fig. 21).

Even though this model is still a crude approximation, as for instance it does not take into account sub-Doppler cooling, higher-order scattering or temperature effects, all known to be important for a MOT of rubidium atoms, it has lead to qualitative new predictions waiting for an experimental investigation. A critical exponent of $\alpha \simeq 0.55$ is for instance predicted for the relaxation time constant $\tau \propto (N_{cr} - N)^{\alpha}$ below the instability threshold, consistent with preliminary experiments. The structure function of the cloud of atoms can also be computed and one can estimate the Coulomb coupling parameter Θ (also called the plasma parameter or correlation parameter), defined as the ratio between the average long-range repulsion
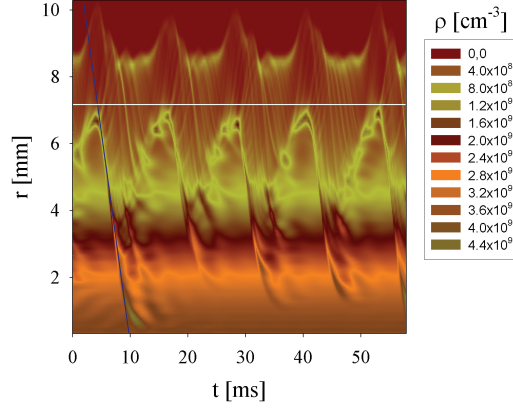
44   *Q. Baudouin, W. Guerin, and R. Kaiser*

Fig. 21.   Spatio-temporal evolution of the density profile (from[169]).

energy and the kinetic energy:[171]

$$\Theta = \frac{q_{\mathrm{eff}}^2}{4\pi\varepsilon_0 a k_{\mathrm{B}} T}. \tag{25}$$

For typical MOTs, this parameter is very small ($\Theta \ll 1$) so that, in order to reach a liquid regime (at $\Theta \sim 2$) or even a crystalline phase (for $\Theta > 170$ in 3 dimensions), one would need to combine these strong long range forces with lower temperatures, which is probably very difficult as this would require small detunings and low temperatures. Nevertheless, this line of research has not be investigated up to now and we point to the possibility of engineering separately the interaction forces by applying an additional low intensity laser beam, tuned close to resonance. We have verified experimentally that this technique allows us to have a time control on the interaction forces and with fine tuning of the parameters, we expect that the Θ parameter could be increased considerably using present cold-atom technologies.

We note that despite differences in the microscopic origin of the long-range forces for radiation pressure in multiple scattering, we expect this system to share many qualitative features with confined one-component plasmas or astrophysical systems. In astrophysics, we expect deeper analogies with our system, as the same radiation pressure forces are at the origin of the balance between compression (mainly due to gravity) and repulsion forces in stars. Without the repulsion force due to radiation pressure, stars

would not be stable and would collapse, which is indeed what happens once their source of radiation is consumed. In this context, it is interesting to note that some stars, called Cepheids, also present very regular oscillations, which make them useful for calibration of distances in the universe. The instabilities of Cepheids also find their driving mechanisms in the outer layer of the system via the so-called κ-mechanism. In this case, the equilibrium between radiation pressure expulsion and radial compression by gravity is perturbed by a radial dependance of the ionization level of elements changing therefore the opacity (κ) of the system.[172] Even though such stellar systems are far more complex than a MOT, it is fascinating that the combination of radiation pressure forces with compression forces can be studied in laboratory experiments. We have for instance explored the potential of driving the MOT below and above the self-induced instability or to use fast CCDs allowing us to observe the evolution of the spatio-temporal structures of a MOT. It should thus be possible to apply various theoretical tools and analyzing methods to a simplified system such as a MOT, allowing a more systematic study of specific properties of these complex models. One could thus study theoretically and experimentally the impact of inelastic scattering in hot atomic vapors (leading to the above discussed Lévy flights) on the radiation pressure force and its balance to compression forces. With only few experimental systems available to study long-range interactions in laboratory conditions, the use of laser-cooled atoms offer an interesting testbed available in many laboratories.

4.3. *Plasma physics with MOTs*

These initial experiments have triggered a line of research, trying to establish in more detail the connection between the physics of long-range interactions, plasma physics and multiple scattering in MOTs. In a more general theoretical study,[173] we have computed the scaling of the frequency of the breathing mode of systems with interaction forces scaling as $1/r^\alpha$. Using a dynamical ansatz in the first equation of the Bogoliubov-Born-Green-Kirkwood-Yvon hierarchy, we have treated a wide range of power-law interactions and interaction strengths, at linear and nonlinear levels. This allowed us to put in a common framework various results scattered in the literature, and by widely generalizing these, to emphasize universal characters of this breathing mode, which can be found in confined plasmas, MOTs and Bose-Einstein condensates, colloidal particles, trapped ions and astrophysical systems. We have obtained analytical results for the scaling
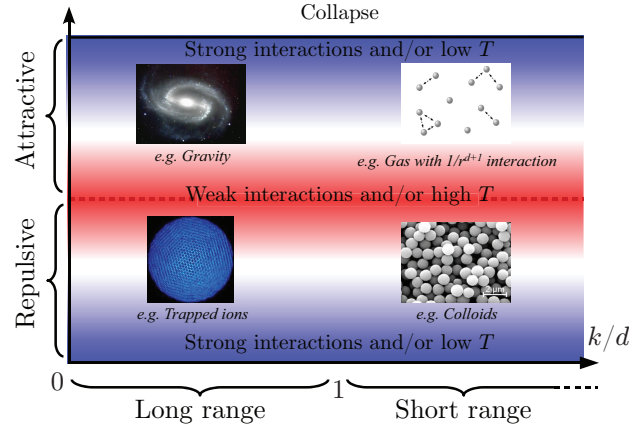
Q. Baudouin, W. Guerin, and R. Kaiser

Fig. 22.   Diagram of the different regimes for the breathing mode. On the horizontal axis, the interaction range, measured by k/d, where k is the exponent of the power-law describing the interaction and d the dimension. The interaction strength is changing along the vertical axis. Pictures of some physical examples are inserted for illustration. Adapted from Ref.[173]

laws, covering both attractive and repulsive, long and short range interactions (Fig. 22). Direct numerical simulations have been used to validate these analytical results.[173] This study has been extended to include space dependent friction and diffusion, indicating a transition from over- to underdamped oscillations.[174] These results show the potential of cold atomic clouds for the study of long-range interacting systems. It will be interesting to explore to what extend light-induced forces could, e.g., be used to realize highly unstable regimes, reminiscent of a kind of optical induced turbulence, which seems to be already included in numerical models (Fig. 21).[169]

Another approach is to use fluid equations as used in plasma physics. This ansatz has been exploited in,[175,176] using both fluid and kinetic equations to describe the collective oscillations in a cloud of neutral atoms confined in a magneto-optical trap. The equations describing the evolution of the atomic gas treated as a fluid are then:

$$\frac{\partial n}{\partial t} + \boldsymbol{\nabla} \cdot (n\boldsymbol{v}) = 0, \tag{26}$$

$$\frac{\partial \boldsymbol{v}}{\partial t} + \boldsymbol{v} \cdot \nabla \boldsymbol{v} = -\frac{\boldsymbol{\nabla} P}{Mn} + \frac{\boldsymbol{F}_{\mathrm{T}}}{M}, \tag{27}$$

where n and $\boldsymbol{v}$ are the density and velocity field of the gas respectively, $\boldsymbol{F}_{\mathrm{T}}$ the total force and P the gas pressure. In order to exploit this approach,

one needs to assume the existence of an equation of state, which has not been measured nor theoretically established by microscopic models. We thus conjecture a relation relating the pressure P of the atomic gas to the temperature T and density n given by an adiabatic equation of the form $P \propto n^{\gamma}$. This approach allows us to derive a dispersion relation for the plasma hybrid waves and eigenmodes of the system, extending the so-called Tonks-Dattner resonances[177,178] to our specific geometry. The dispersion relation shows the presence of an acoustic mode for large wavevectors with a crossover into electron-plasma-like wave for small wavevectors. The validity of this dispersion relation could be verified in experiments by a convenient modulation of the MOT and the detection of propagating waves from the source of modulation. Another result of this analysis is the computation of the excitation spectra and an analysis of the eigenmodes of the oscillations of the systems. We have obtained the nodes of the eigenstates of the cloud for different excitation energies.[175] We thus perform a kind of seismology of MOTs similar to asteroseismology.[179]

4.4. *Opto-mechanical instabilities*

So far we have only considered the action of multiply-scattered light onto the motion of the atom. However, it is also possible to consider a feedback of the motion of atoms onto the propagation of light. In cold atoms, such a feedback scheme is typically considered for atomic clouds located in an optical cavity, enhancing the coupling between the atoms and the light mode.[126,127,148,180,181] Only recently one experiment has observed opto-mechanical instabilities in the absence of an external cavity.[182] All these experiments are based on the use of dipole forces and the propagation of light is considered to be determined by diffraction of the field on the index profile provide by the atoms. However different opto-mechanical coupling schemes can be considered two regimes of light propagation (diffraction or multiple scattering) and two types of forces (dipole force or radiation pressure force) can be combined.

In astrophysical context, the propagation of light has been considered by a fluid description, resulting in a set of two coupled-fluid equations: one for the light and one for the matter. If the forces on the matter are strong enough (such as close to extreme sources of radiation), even a hot cloud of atoms is expected to be expelled by the extreme radiation. This leads to regions void of matter, allowing the radiation to propagate freely. A simple picture of this coupling is the presence of bubbles of light, from which

48   *Q. Baudouin, W. Guerin, and R. Kaiser*

the matter is expelled. Such so-called photon bubbles[183–185] are another example of the impact of radiation pressure in astrophysical systems. With the advent of laser-cooled atoms, it is now possible to study the radiation pressure forces in a large variety of regime. We have thus explored the possibility of combining an equation for the propagation of light in the multiple scattering limit with the radiation pressure forces on cold atoms.[186] In the simplest model, we have used a diffusion equation for the propagation of light and a fluid equation for the distribution of the atoms. The coupling between these two equations is included in the diffusion equation in the fact that the photon mean free path and thus the diffusion coefficient depends on the atomic density. The fluid equation depends on the evolution of the light field via the local intensity, which gives rise to the repulsion force between the atoms (described by an effective charge in the fluid equation).

Using a linear stability ansatz, we have identified two types of photon bubbles in cold atoms: oscillating bubbles and purely growing bubbles.[186] We stress that this set of coupled equations gives rise to opto-mechanical instabilities even in the limit of low light intensity, where the electronic nonlinearity of the atomic response is not relevant. The nonlinearity is provided by the mechanical response of the atoms changing the diffusion coefficient for the propagation of light.

It is intriguing to notice that in our test particle model outlined above,[169] we had already observed spatio-temporal structures. However this model assumed a spherical symmetry of the atomic density. It would thus be interesting to extend this test particle model to 2 or 3 dimensions and validate the possibility of photon bubbles in cold-atom clouds. An experimental observation of photon bubbles should also be possible. When tuning the MOT parameters to regime deep inside the instability region, we have observed complex spatio-temporal structures. Looking for photon bubbles in this regime requires a more systematic study of these structures and it might be possible to relate them to optically-induced turbulence.

4.5. *Outlook*

As outlined above the study of long range forces in cold atomic clouds allows for qualitative new features to be explored. Despite the relative simple experimental setup and the large number of predictions, only few systematic experiments have been conducted. Based on the expertise obtained from experiments conducted in our group in Nice, we conjecture that several of the predictions above should be possible to observe in cold-atom

Cold and hot atomic vapors: a testbed for astrophysics?   49

experiments. We can also outline a few promising directions, which deserve further investigation.

First, the concept of long-range interacting systems could be extended to the description of the internal degrees of freedom of the atoms. In this work, we have focused on the external degrees of freedom (position and momentum of the atoms), but in a different line of research, we have studied how global coupling between the atoms affect their internal degrees of freedom (their polarizability): we have indeed found that such long-range global coupling can drastically change the physics of light propagation in disordered systems, to a point where phase transitions (such as Anderson localization of light) need to be analyzed with a different approach.[26] It would for instance be interesting to see if the inequivalence between a micro-canonical and a canonical description of the system would lead to different phase transitions. The possibility of quasi-stationary states in long-range interacting systems have been considered for gravitational interactions, but not yet for resonant dipole interactions.

Concerning the relation to plasma physics, it would be interesting to have a quantitative understanding of the differences and similarities between the mechanisms of the "Seoul",[160–163] "Lille"[164–166] and "Nice"[168–170] instabilities. Experiments comparing retroreflected and six-beam geometry and analyzing the impact of a sub-Doppler MOT component seem possible and should allow to solve some remaining controversies.[166]

One important result would be the observation of the equivalent of a Debye length of atoms in presence of long-range interactions. As in one-component plasmas, we do indeed expect that atoms will repel each other at short distances (leading to a kind of exclusion or Wigner-Seitz radius), but at a larger scale atoms can organize themselves in a non-trivial arrangement of positions, which a spatial correlation function described by a Debye screening length λ_D. The observation of such Debye screening via, e.g., diffraction of a probe beam, requires an excellent signal to noise ratio, as only few atoms will be contained in a volume of λ_D^3.

Also, the measurement of a dispersion relation of the atomic fluid could be realized by a time-dependant perturbation of part of the atomic cloud.

Another promising project is to make use of dipole forces to induce repulsive or attractive interatomic interactions. Such dipole forces are present in a local speckle field but can also be obtained with low optical thickness, realizing en equivalent of optical binding[146,147] with cold atoms. Such experiments can also be considered as light-induced pattern formation or

50   *Q. Baudouin, W. Guerin, and R. Kaiser*

self-organization of atoms, extending existing experiments[148,182] into novel regimes.

5. Conclusion

In this chapter, we have presented several experiments dealing with multiple scattering of light in atomic vapors. This topic, on which our group in Nice has been focussed for now 15 years, is richer than what has been presented here. In particular, two important subjects have not been discussed. The first one, that we extensively studied in the past (see the reviews[187,188]), is the decoherence of the optical wave during the multiple-scattering process, which can be probed by the coherent-backscattering effect. The second, more recent subject, is the role of cooperative effects (such as Dicke super-radiance and subradiance,[189,190] single-photon superradiance,[191] collective Lamb shift[192,193]) on light-atom interaction, light transport in cold atoms and disorder-induced localization effects (see, e.g., Refs.[26,194–197]). Possible connections between such coherence effects and astrophysical observations seem too premature and would need more thorough investigation.

The connections between astrophysical systems and the effects that we discussed here, namely radiation trapping, Lévy flights, random lasing, and long-range light-induced forces, would also need to be studied more deeply. To this end, our purpose here is to stimulate more interdisciplinary exchange between research communities of cold atoms, plasma physics, long-range interacting systems and astrophysics.

Finally, note that there are other astrophysical effects, not based on multiple scattering of light, which can also be investigated using analogies in cold-atom physics, such as neutron stars (using degenerate Fermi gases),[198] supernova (using unstable Bose-Einstein condensates with negative scattering length),[199,200] Hawking radiation (using sound waves in superfluid gases),[201–203] and other general-relativity effects.[204] Although they are beyond the scope of this chapter, they also contribute to showing that cold-atom physics and astrophysics can have much in common.

Cold and hot atomic vapors: a testbed for astrophysics? 51

References

1. C. Cohen-Tannoudji and D. Guéry-Odelin, *Advances in atomic physics: an overview*. World Scientific, Singapour (2011).
2. H. Metcalf and P. van der Straten, *Laser cooling and Trapping*. Springer, New York (1999).
3. V. S. Letokhov and S. Johansson, *Astrophysical Lasers*. Oxford University Press (2009).
4. K. T. Compton, Theory of ionization by cumulative action and the low voltage arc, *Phys. Rev.* **20**, 283–299 (1922).
5. K. T. Compton, Some properties of resonance radiation and excited atoms, *Philos. Mag.* **45**, 752 (1923).
6. M. W. Zemansky, The diffusion of imprisoned resonance radiation in mercury vapor, *Phys. Rev.* **29**, 513–523 (1927).
7. C. Kenty, On radiation diffusion and the rapidity of escape of resonance radiation from a gas, *Phys. Rev.* **42**, 823–842 (1932).
8. T. Holstein, Imprisonment of resonance radiation in gases, *Phys. Rev.* **72**, 1212–1233 (1947).
9. R. N. Thomas, The source function in a non-equilibrium atmosphere. I. The resonance lines, *ApJ.* **125**, 260 (1957).
10. J. T. Jefferies and R. N. Thomas, The source function in a non-equilibrium atmosphere. II. The depth dependence of the source function for resonance and strong subordinate lines, *ApJ.* **127**, 667 (1958).
11. R. N. Thomas, The source function in a non-equilibrium atmosphere. IV. Evaluation and applications of the net radiative bracket, *ApJ.* **131**, 429 (1960).
12. R. Kaiser. Cold atoms and multiple scattering. In eds. R. Kaiser and J. Montaldi, *Peyresq Lectures on Nonlinear Phenomena*. World Scientific, Singapour (2000).
13. A. Lagendijk and B. A. van Tiggelen, Resonant multiple scattering of light, *Phys. Rep.* **270**, 143–215 (1996).
14. P. de Vries, D. V. van Coevorden, and A. Lagendijk, Point scatterers for classical waves, *Rev. Mod. Phys.* **70**, 447–466 (1998).
15. G. Labeyrie, D. Delande, C. A. Müller, C. Miniatura, and R. Kaiser, Multiple scattering of light in a resonant medium, *Opt. Commun.* **243**, 157–164 (2004).
16. M. C. W. van Rossum and T. M. Nieuwenhuizen, Multiple scattering of classical waves: microscopy, mesoscopy, and diffusion, *Rev. Mod. Phys.* **71**,

52   *Q. Baudouin, W. Guerin, and R. Kaiser*

313–371 (1999).

17. A. Molisch and B. Oehry, *Radiation Trapping in Atomic Vapours*. Oxford University Press (1998).

18. A. Fioretti, A. F. Molisch, J. H. Mutter, P. Verkerk, and M. Allegrini, Observation of radiation trapping in a dense Cs magneto-optical trap, *Opt. Commun.* **149**, 415–422 (1998).

19. G. Labeyrie, E. Vaujour, C. A. Müller, D. Delande, C. Miniatura, D. Wilkowski, and R. Kaiser, Slow diffusion of light in a cold atomic cloud, *Phys. Rev. Lett.* **91**, 223904 (2003).

20. G. Labeyrie, R. Kaiser, and D. Delande, Radiation trapping in a cold atomic gas, *Appl. Phys. B.* **81**, 1001–1008 (2005).

21. R. Pierrat, B. Grémaud, and D. Delande, Enhancement of radiation trapping for quasiresonant scatterers at low temperature, *Phys. Rev. A.* **80**, 013831 (2009).

22. T. Jonckheere, C. A. Müller, R. Kaiser, C. Miniatura, and D. Delande, Multiple scattering of light by atoms in the weak localization regime, *Phys. Rev. Lett.* **85**, 4269 (2000).

23. G. Labeyrie, C. Miniatura, C. A. Müller, O. Sigwarth, D. Delande, and R. Kaiser, Hanle effect in coherent backscattering, *Phys. Rev. Lett.* **89**, 163901 (2002).

24. C. A. Müller and C. Miniatura, Multiple scattering of light by atoms with internal degeneracy, *J. Phys. A: Math. Gen.* **35**, 10163–10188 (2002).

25. G. Labeyrie, F. de Tomasi, J.-C. Bernard, C. A. Müller, C. Miniatura, and R. Kaiser, Coherent backscattering of light by cold atoms, *Phys. Rev. Lett.* **83**, 5266–5269 (Dec, 1999).

26. E. Akkermans, A. Gero, and R. Kaiser, Photon localization and Dicke superradiance in atomic gases, *Phys. Rev. Lett.* **101**, 103602 (2008).

27. S. E. Skipetrov and I. M. Sokolov, Absence of Anderson localization of light in a random ensemble of point scatterers, *Phys. Rev. Lett.* **112**, 023905 (2014).

28. Q. Baudouin, N. Mercadier, and R. Kaiser, Steady-state signatures of radiation traping by cold multilevel atoms, *Phys. Rev. A.* **87**, 013412 (2013).

29. P. Lévy, *Théorie de l'addition des variables aléatoires*. Gauthier-Villiers (1937).

30. J.-P. Bouchaud and A. Georges, Anomalous diffusion in disordered media: statistical mechanisms, models and physical applications, *Phys. Rep.* **195**, 127–293 (1990).

31. M. Shlesinger, G. Zaslavsky, and U. Frisch, *Lévy flights and related topics in physics*. Springer (1995).

32. R. Metzler and J. Klafter, The random walk's guide to anomalous diffusion: a fractional dynamics approach, *Phys. Rep.* **339**, 1–77 (2000).

33. J.-P. Bouchaud and M. Potters, *Theory of financial risk and derivative pricing*. Cambridge Univ. Press (2003).

34. R. Botet and M. Ploszajczak, *Universal fluctuations*. World Scientific (2002).

35. N. D. Goldenfeld, *Lectures on phase transitions and the renormalisation*

Cold and hot atomic vapors: a testbed for astrophysics?   53

group. Addison (1992).

36. P. Barthelemy, J. Bertolotti, and D. S. Wiersma, A Lévy flight for light, *Nature.* **453**, 495–498 (2008).

37. U. Springmann, Multiple resonance line scattering and the momentum problem in Wolf-Rayet star winds, *A& A.* **289**, 505–523 (1994).

38. E. Pereira, J. M. G. Martinho, and M. N. Berberan-Santos, Photon trajectories in incoherent atomic radiation trapping as Lévy flights, *Phys. Rev. Lett.* **93**, 120201 (2004).

39. M. Burresi, V. Radhalakshmi, R. Savo, J. Bertolotti, K. Vynck, and D. S. Wiersma, Weak localization of light in superdiffusive random systems, *Phys. Rev. Lett.* **108**, 110604 (2012).

40. C. W. Groth, A. R. Akhmerov, and C. W. J. Beenakker, Transmission probability through a Lévy glass and comparison with a Lévy walk, *Phys. Rev. E.* **85**, 021138 (2012).

41. R. Burioni, S. di Santo, S. Lepri, and A. Vezzani, Scattering lengths and universality in superdiffusive Lévy materials, *Phys. Rev. E.* **86**, 031125 (2012).

42. N. Mercadier, W. Guerin, M. Chevrollier, and R. Kaiser, Lévy flights of photons in hot atomic vapors, *Nature Phys.* **5**, 602 (2009).

43. M. Chevrollier, N. Mercadier, W. Guerin, and R. Kaiser, Anomalous photon diffusion in atomic vapors, *Eur. Phys. J. D.* **58**, 161 (2010).

44. N. Mercadier, M. Chevrollier, W. Guerin, and R. Kaiser, Microscopic characterization of Lévy flights of light in atomic vapors, *Phys. Rev. A.* **87**, 063837 (2013).

45. M. Chevrollier, Radiation trapping and Lévy flights in atomic vapours: an introductory review, *Contemp. Phys.* **53**, 227–239 (2012).

46. Q. Baudouin, R. Pierrat, A. Eloy, E. J. Nunes-Pereira, P. Cuniasse, N. Mercadier, and R. Kaiser, Signatures of lévy flights with annealed disorder (2014). arXiv:1402.6200.

47. I. Millic and M. Faurobert, Modeling scattering polarization in molecular solar lines in spherical geometry, *A&A.* **539**, 10 (2012).

48. G. Labeyrie, C. Miniatura, and R. Kaiser, Large Faraday rotation of resonant light in a cold atomic cloud, *Phys. Rev. A.* **64**, 033402 (2001).

49. R. P. Eatough et al., A strong magnetic field around the supermassive black hole at the center of the galaxy, *Nature.* **501**, 391–394 (2013).

50. V. M. Datsyuk, I. M. Sokolov, D. V. Kupriyanov, and M. D. Havey, Diffuse light scattering dynamics under conditions of electromagnetically induced transparency, *Phys. Rev. A.* **74**, 043812 (2006).

51. V. S. Letokhov, Generation of light by a scattering medium with negative resonance absorption, *Sov. Phys. JETP.* **26**, 835–840 (1968).

52. H. Cao, Lasing in random media, *Waves Random Media.* **13**, R1–R39 (2003).

53. V. M. Markushev, V. F. Zolin, and C. M. Briskina, Luminescence and stimulated emission of neodymium in sodium lanthanum molybdate powders, *Sov. J. Quantum Electron.* **16**, 281–282 (1986).

54. C. Gouedard, D. Husson, D. Sauteret, F. Auzel, and A. Migus, Generation of spatially incoherent short pulses in laser-pumped neodymium stoichiometric

54 *Q. Baudouin, W. Guerin, and R. Kaiser*

crystals and powders, *J. Opt. Soc. Am. B.* **10**, 2358–2362 (1993).

55. N. M. Lawandy, R. M. Balachandran, A. S. L. Gomes, and E. Sauvain, Laser action in strongly scattering media, *Nature.* **368**, 436–438 (1994).

56. H. Cao, Y. G. Zhao, H. C. Ong, S. T. Ho, J. Y. Dai, J. Y. Wu, and R. P. H. Chang, Ultraviolet lasing in resonators formed by scattering in semiconductor polycrystalline films, *Appl. Phys. Lett.* **73**, 3656–3658 (1998).

57. H. Cao, Y. G. Zhao, S. T. Ho, E. W. Seeling, Q. H. Wang, and R. P. H. Chang, Random laser action in semiconductor powder, *Phys. Rev. Lett.* **82**, 2278–2281 (1999).

58. D. S. Wiersma and S. Cavalier, Light emission: A temperature-tunable random laser, *Nature.* **414**, 708–709 (2001).

59. G. Strangi, S. Ferjani, V. Barna, A. D. Luca, C. Versace, N. Scaramuzza, and R. Bartolino, Random lasing and weak localization of light in dye-doped nematic liquid crystals, *Opt. Express.* **14**, 7737–7744 (2006).

60. S. Gottardo, R. Sapienza, P. D. García, A. Blanco, D. S. Wiersma, and C. López, Resonance-driven random lasing, *Nature Photon.* **2**, 429–432 (2008).

61. J. Fallert, R. J. B. Dietz, J. Sartor, D. Schneider, C. Klingshirn, and H. Kalt, Co-existence of strongly and weakly localized random laser modes, *Nature Photon.* **3**, 279–282 (2009).

62. J. Andreasen, A. A. Asatryan, L. C. Botten, M. A. Byrne, H. Cao, L. Ge, L. Labonté, P. Sebbah, A. D. Stone, H. E. Türeci, and C. Vanneste, Modes of random lasers, *Adv. Opt. Photon.* **3**, 88–127 (2011).

63. D. S. Wiersma, Disordered photonics, *Nature Photon.* **7**, 188–196 (2013).

64. D. S. Wiersma and A. Lagendijk, Light diffusion with gain and random lasers, *Phys. Rev. E.* **54**, 4256–4265 (1996).

65. A. L. Burin, M. A. Ratner, H. Cao, and R. P. H. Chang, Model for a random laser, *Phys. Rev. Lett.* **87**, 215503 (2001).

66. C. Vanneste, P. Sebbah, and H. Cao, Lasing with resonant feedback in weakly scattering random systems, *Phys. Rev. Lett.* **98**, 143902 (2007).

67. H. E. Türeci, L. Ge, S. Rotter, and A. D. Stone, Strong interactions in multimode random lasers, *Science.* **320**, 643–646 (2008).

68. C. Conti and A. Fratalocchi, Dynamic light diffusion, three-dimensional Anderson localization and lasing in inverted opals, *Nature Phys.* **4**, 794–798 (2008).

69. R. Frank, A. Lubatsch, and J. Kroha, Light transport and localization in diffusive random lasers, *J. Opt. A: Pure Appl. Opt.* **11**, 114012 (2009).

70. A. Goetschy and S. E. Skipetrov, Euclidean matrix theory of random lasing in a cloud of cold atoms, *Europhys. Lett.* **96**, 34005 (2011).

71. D. S. Wiersma, The physics and applications of random lasers, *Nature Phys.* **4**, 359–367 (2008).

72. B. Redding, M. A. Choma, and H. Cao, Speckle-free laser imaging using random laser illumination, *Nature Photon.* **6**, 355–359 (2012).

73. Q. Baudouin, N. Mercadier, V. Guarrera, and R. Kaiser, A cold-atom random laser, *Nature Phys.* **9**, 357–360 (2013).

74. H. Weaver, D. R. W. Williams, N. H. Dieter, and W. T. Lum, Observa-

tions of a strong unidentified microwave line and of emission from the OH molecule, *Nature.* **208**, 29–31 (1965).

75. M. M. Litvak, A. L. McWhorter, M. L. Meeks, and H. J. Zeiger, Maser model for interstellar OH microwave emission, *Phys. Rev. Lett.* **17**, 821–826 (1966).

76. M. J. Reid and J. M. Moran, Masers, *Ann. Rev. Astron. Astrophys.* **19**, 231–276 (1981).

77. M. Elitzur, Physical characteristics of astronomical masers, *Rev. Mod. Phys.* **54**, 1225–1260 (1982).

78. A. D. Thackerey, The emission line λ4511 in late-type variables, *ApJ.* **81**, 467–473 (1935).

79. P. W. Merrill, *Lines of the Chemical Elements in Astronomical Spectra.* Carnegie Institution of Washington (1956).

80. V. S. Letokhov, Laser action in stellar atmospheres, *IEEE J. Quantum. Electron.* **8**, 615 (1972).

81. N. N. Lavrinovich and V. S. Letokhov, The possibility of the laser effect in stellar atmospheres, *Sov. Phys. JETP.* **40**, 800–805 (1975).

82. M. A. Johnson, M. A. Betz, R. A. McLaren, E. C. Sutton, and C. H. Townes, Nonthermal 10 micron CO_2 emission lines in the atmospheres of Mars and Venus, *ApJ.* **208**, L145–L148 (1976).

83. M. J. Mumma, D. Buhl, G. Chin, D. Deming, F. Espenak, T. Kostiuk, and D. Zipoy, Discovery of natural gain amplification in the 10-micrometer carbon dioxide laser bands on Mars: a natural laser, *Science.* **212**, 45–49 (1981).

84. V. S. Strelnitski, M. R. Haas, H. A. Smith, E. F. Erickson, S. W. J. Colgan, and D. J. Hallenbach, Far-infrared hydrogen lasers in the peculiar star MWC 349A, *Science.* **272**, 1459–1461 (1996).

85. S. Johansson and V. S. Letokhov, Astrophysical lasers operating in optical Fe II lines in stellar ejecta of η carinae, *A&A.* **428**, 497–509 (2004).

86. S. Johansson and V. S. Letokhov, Astrophysical laser operating in the O I 8446-Å line in the weigelt blobs of η Carinae, *Mon. Not. Roy. Astron. Soc.* **364**, 731–737 (2005).

87. S. J. Messenger and V. Strelnitski, On the 1.7 μm Fe II and other natural lasers, *Mon. Not. Roy. Astron. Soc.* **404**, 1545–1550 (2010).

88. T. Shimoikura, H. Kobayashi, T. Omodaka, P. J. Diamond, L. I. Matveyenko, and K. Fujisawa, VLBA observations of a bursting water maser in Orion KL, *ApJ.* **634**, 459–467 (2005).

89. P. Truitt and V. Strelnitski, Transition to oscillation regime in flaring water vapour masers, *Bull. Am. Astron. Soc.* **32**, 1484 (2000).

90. T. Hirota, M. Tsuboi, K. Fujisawa, M. Honma, N. Kawaguchi, M. K. Kim, H. Kobayashi, H. Imai, T. Omodaka, K. M. Shibata, T. Shimoikura, and Y. Yonekura, Identification of bursting water maser features in Orion KL, *ApJ.* **739**, L59 (2011).

91. S. Johansson and V. S. Letokhov, Astrophysical lasers and nonlinear optical effects in space, *New. Astron. Rev.* **51**, 443–523 (2007).

92. D. Dravins. Photonic astronomy and quantum optics. In eds. D. Phelan,

56   *Q. Baudouin, W. Guerin, and R. Kaiser*

O. Ryan, and A. Shearer, *High Time Resolution Astrophysics*, vol. 351, *Astrophysics and Space Science Library*. Springer, Berlin (2008).

93. C. Cohen-Tannoudji, J. Dupont-Roc, and G. Grynberg, *Atom-Photon Interactions: Basic Processes and Applications*. Wiley, New York (1992).

94. W. Guerin, N. Mercadier, F. Michaud, D. Brivio, L. S. Froufe-Pérez, R. Carminati, V. Eremeev, A. Goetschy, S. E. Skipetrov, and R. Kaiser, Towards a random laser with cold atoms, *J. Opt.* **12**, 024002 (2010).

95. B. R. Mollow, Stimulated emission and absorption near resonance for driven systems, *Phys. Rev. A.* **5**, 2217–2222 (1972).

96. F. Y. Wu, S. Ezekiel, M. Ducloy, and B. R. Mollow, Observation of amplification in a strongly driven two-level atomic system at optical frequencies, *Phys. Rev. Lett.* **38**, 1077–1080 (1977).

97. G. Grynberg and C. Cohen-Tannoudji, Central resonance of the Mollow absorption spectrum: physical origin of gain without population inversion, *Opt. Commun.* **96**, 150–163 (1993).

98. J. Zakrzewski, Theoretical explanation of the first experimentally observed laser without inversion in a two-level scheme, *Phys. Rev. A.* **46**, 6010–6014 (1992).

99. J. Mompart and R. Corbalán, Lasing without inversion, *J. Opt. B: Quantum Semiclass. Opt.* **2**, R7–R24 (2000).

100. W. Guerin, F. Michaud, and R. Kaiser, Mechanisms for lasing with cold atoms as the gain medium, *Phys. Rev. Lett.* **101**, 093002 (2008).

101. J. W. R. Tabosa, G. Chen, Z. Hu, R. B. Lee, and H. J. Kimble, Nonlinear spectroscopy of cold atoms in a spontaneous-force optical trap, *Phys. Rev. Lett.* **66**, 3245–3248 (1991).

102. D. Grison, B. Lounis, C. Salomon, J.-Y. Courtois, and G. Grynberg, Raman spectroscopy of cesium atoms in a laser trap, *Europhys. Lett.* **15**, 149–154 (1991).

103. T. M. Brzozowski, M. Brzozowska, J. Zachorowski, M. Zawada, and W. Gawlik, Probe spectroscopy in an operating magneto-optical trap: The role of raman transitions between discrete and continuum atomic states, *Phys. Rev. A.* **71**, 013401 (2005).

104. L. Hilico, C. Fabre, and E. Giacobino, Operation of a "cold-atom laser" in a magneto-optical trap, *Europhys. Lett.* **18**, 685–688 (1992).

105. J. McKeever, A. Boca, A. D. Boozer, J. R. Buck, and H. J. Kimble, Experimental realization of a one-atom laser in the regime of strong coupling, *Nature.* **425**, 268–271 (2003).

106. G. Vrijsen, O. Hosten, J. Lee, S. Bernon, and M. A. Kasevich, Raman lasing with a cold atom gain medium in a high-finesse optical cavity, *Phys. Rev. Lett.* **107**, 063904 (2011).

107. J. G. Bohnet, Z. Chen, J. M. Weiner, D. Meiser, M. J. Holland, and J. K. Thompson, A steady-state superradiant laser with less than one intracavity photon, *Nature.* **484**, 78–81 (2012).

108. A. Yariv and D. M. Pepper, Amplified reflection, phase conjugation, and oscillation in degenerate four-wave mixing, *Opt. Lett.* **1**, 16–18 (1977).

109. R. L. Abrams and R. C. Lind, Degenerate four-wave mixing in absorbing

Cold and hot atomic vapors: a testbed for astrophysics?   57

media, *Opt. Lett.* **2**, 94–96 (1978). Errata, *Opt. Lett.* **3**, 205 (1978).

110. R. W. Boyd, M. G. Raymer, P. Narum, and D. J. Harter, Four-wave parametric interactions in a strongly driven two-level system, *Phys. Rev. A.* **24**, 411–423 (1981).

111. A. Schilke, C. Zimmermann, P. W. Courteille, and W. Guerin, Optical parametric oscillation with distributed feedback in cold atoms, *Nature Photon.* **6**, 101 (2012).

112. B. Kleinmann, F. Trehin, M. Pinard, and G. Grynberg, Degenerate four-wave mixing in sodium vapor in the Rabi regime, *J. Opt. Soc. Am. B.* **2**, 704–713 (1985).

113. M. Pinard, D. Grandclement, and G. Grynberg, Continuous-wave self-oscillation using pair production of photons in four-wave mixing in sodium, *Europhys. Lett.* **2**, 755–760 (1986).

114. M. R. R. Leite, P. Simoneau, D. Bloch, S. Le Boiteux, and M. Ducloy, Continuous-wave phase-conjugate self-oscillation induced by Na-vapour degenerate four-wave mixing with gain, *Europhys. Lett.* **2**, 747–753 (1986).

115. F. Michaud, G.-L. Gattobigio, J. W. R. Tabosa, and R. Kaiser, Interference between Raman gain and four-wave mixing in cold atoms, *J. Opt. Soc. Am. B.* **24**, A40–A47 (2007).

116. R. C. Lind and D. G. Steel, Demonstration of the longitudinal modes and aberration correction properties of a continuous-wave dye laser with a phase-conjugate mirror, *Opt. Lett.* **6**, 554–556 (1981).

117. A. Schilke. *Photonische Eigenschaften eines eindimensionalen geordneten atomaren Mediums.* PhD thesis, Eberhard-Karls-Universität Tübingen (2013).

118. N. Mercadier. *Diffusion résonante de la lumière: laser aléatoire à atomes et vols de Lévy des photons.* PhD thesis, Université Nice Sophia Antipolis (2011).

119. G. G. Padmabandu, G. R. Welch, I. N. Shubin, E. S. Fry, D. E. Nikonov, M. D. Lukin, and M. O. Scully, Laser oscillation without population inversion in a sodium atomic beam, *Phys. Rev. Lett.* **76**, 2053–2056 (1996).

120. A. S. Zibrov, M. D. Lukin, D. E. Nikonov, L. Hollberg, M. O. Scully, V. L. Velichansky, and H. G. Robinson, Experimental demonstration of laser oscillation without population inversion via quantum interference in Rb, *Phys. Rev. Lett.* **75**, 1499–1502 (1995).

121. J. Kitching and L. Hollberg, Interference-induced optical gain without population inversion in cold, trapped atoms, *Phys. Rev. A.* **59**, 4685–4689 (1999).

122. J.-Y. Courtois, G. Grynberg, B. Lounis, and P. Verkerk, Recoil-induced resonances in cesium: An atomic analog to the free-electron laser, *Phys. Rev. Lett.* **72**, 3017–3020 (1994).

123. M. Vengalattore and M. Prentiss, Recoil-induced resonances in the high-gain regime, *Phys. Rev. A.* **72**, 021401 (2005).

124. R. Bonifacio and L. De Salvo, Collective atomic recoil laser (CARL): optical gain without inversion by collective atomic recoil and self-bunching of two-level atoms, *Nucl. Instrum. Methods Phys. Res. Sect. A.* **341**, 360 – 362 (1994).

58   *Q. Baudouin, W. Guerin, and R. Kaiser*

125. P. R. Berman, Comparison of recoil-induced resonances and the collective atomic recoil laser, *Phys. Rev. A.* **59**, 585–596 (1999).

126. D. Kruse, C. von Cube, C. Zimmermann, and P. W. Courteille, Observation of lasing mediated by collective atomic recoil, *Phys. Rev. Lett.* **91**, 183601 (2003).

127. S. Slama, S. Bux, G. Krenz, C. Zimmermann, and P. W. Courteille, Superradiant rayleigh scattering and collective atomic recoil lasing in a ring cavity, *Phys. Rev. Lett.* **98**, 053603 (2007).

128. D. J. Gauthier, Q. Wu, S. E. Morin, and T. W. Mossberg, Realization of a continuous-wave, two-photon optical laser, *Phys. Rev. Lett.* **68**, 464–467 (1992).

129. K. Case and P. Zweifel, *Linear transport theory.* Addison-Wesley, Reading, MA (1967).

130. K. Drozdowicz, E. Krynicka, and J. Dąbrowska, Diffusion cooling of thermal neutrons in basic rock minerals by monte carlo simulation of the pulsed neutron experiments, *App. Rad. Isot.* **58**, 727–733 (2003).

131. S. Chandrasekhar, *Radiative Transfer.* Dover, New York (1960).

132. R. Elaloufi, R. Carminati, and J.-J. Greffet, Diffusive-to-ballistic transition in dynamic light transmission through thin scattering slabs: a radiative transfer approach, *J. Opt. Soc. Am. B.* **21**, 1430–1437 (2004).

133. R. Pierrat and R. Carminati, Threshold of random laser in the incoherent transport regime, *Phys. Rev. A.* **76**, 023821 (2007).

134. L. S. Froufe-Pérez, W. Guerin, R. Carminati, and R. Kaiser, Threshold of a random laser with cold atoms, *Phys. Rev. Lett.* **102**, 173903 (2009).

135. V. V. Sobolev, *A treatise on Radiative Transfer.* D. Van Nostrand Co., Inc (1963).

136. W. Unno and E. A. Spiegel, The Eddington approximation in the radiative heat equation, *Publ. Astron. Soc. Jpn.* **18**, 85–95 (1966).

137. Y. Kawata and W. M. Irvine, The Eddington approximation for planeteray atmospheres, *ApJ.* **160**, 787–790 (1970).

138. W. J. Wiscombe and J. H. Joseph, The range of validity of the Eddington approximation, *Icarus.* **32**, 362–377 (1977).

139. J. D. Jackson, *Classical Electrodynamics*, 3 edn. Wiley, New York (1999).

140. W. Guerin, N. Mercadier, D. Brivio, and R. Kaiser, Threshold of a random laser based on Raman gain in cold atoms, *Opt. Express.* **17**, 11236 (2009).

141. P. Kumar and J. H. Shapiro, Observation of Raman-shifted oscillation near the sodium D lines, *Opt. Lett.* **10**, 226–228 (1985).

142. F. Bouchet and J. Barré, Classification of phase transitions and ensemble inequivalence in systems with long range interactions, *J. Stat. Phys.* **118**, 1073–1105 (2005).

143. J. Barré, F. Bouchet, T. Dauxois, and S. Ruffo, Large deviation techniques applied to systems with long-range interactions, *J. Stat. Phys.* **119**, 677–713 (2005).

144. M. S. Longair, *Galaxy Formation.* Springer (1998).

145. T. Dauxois, S. Ruffo, and L. F. Cugliandolo, eds., *Long-Range Interacting Systems.* vol. 90, *Lecture Notes of the Les Houches Summer School*, Oxford

Cold and hot atomic vapors: a testbed for astrophysics?   59

University Press (2010).

146. M. M. Burns, J.-M. Fournier, and J. A. Golovchenko, Optical binding, *Phys. Rev. Lett.* **63**, 1233–1236 (1989).

147. K. Dholakia and P. Zemánek, *Colloquium* : Gripped by light: Optical binding, *Rev. Mod. Phys.* **82**, 1767–1791 (2010).

148. H. Ritsch, P. Domokos, F. Brennecke, and T. Esslinger, Cold atoms in cavity-generated dynamical optical potentials, *Rev. Mod. Phys.* **85**, 553–601 (2013).

149. G. Sagué, E. Vetsch, W. Alt, D. Meschede, and A. Rauschenbeutel, Cold-atom physics using ultrathin optical fibers: Light-induced dipole forces and surface interactions, *Phys. Rev. Lett.* **99**, 163602 (2007).

150. M. Lewenstein, A. Sanpera, V. Ahufinger, B. Damskic, A. Sen(De), and U. Sen, Ultracold atomic gases in optical lattices: mimicking condensed matter physics and beyond, *Adv. Phys.* **56**, 243–379 (2007).

151. M. Greiner, O. Mandel, T. Esslinger, T. W. Hänsch, and I. Bloch, Quantum phase transition from a superfluid to a Mott insulator in a gas of ultracold atoms, *Nature.* **415**, 39–44 (2002).

152. K. Góral, L. Santos, and M. Lewenstein, Quantum phases of dipolar bosons in optical lattices, *Phys. Rev. Lett.* **88**, 170406 (2002).

153. J. Dalibard, Laser cooling of an optically thick gas: the simplest radiation pressure trap?, *Opt. Commun.* **68**, 203 (1988).

154. R. P. Feynman, *Feynman Lectures on Gravitation.* Addison-Wesley (1995).

155. T. Walker, D. Sesko, and C. Wieman, Collective behavior of optically trapped neutral atoms, *Phys. Rev. Lett.* **64**, 408–411 (1990).

156. L. Pruvost, I. Serre, H. T. Duong, and J. Jortner, Expansion and cooling of a bright rubidium three-dimensional optical molasses, *Phys. Rev. A.* **61**, 053408 (2000).

157. C. G. Townsend, N. H. Edwards, C. J. Cooper, K. P. Zetie, C. J. Foot, A. M. Steane, P. Szriftgiser, H. Perrin, and J. Dalibard, Phase-space density in the magneto-optical trap, *Phys. Rev. A.* **52**, 1423–1440 (1995).

158. G.-L. Gattobigio, T. Pohl, G. Labeyrie, and R. Kaiser, Scaling laws for large magneto-optical traps, *Phys. Scr.* **81**, 025301 (2010).

159. W. Ketterle, K. B. Davis, M. A. Joffe, A. Martin, and D. E. Pritchard, High densities of cold atoms in a *dark* spontaneous-force optical trap, *Phys. Rev. Lett.* **70**, 2253 (1993).

160. K. Kim, H.-R. Noh, Y.-H. Yeon, and W. Jhe, Observation of the Hopf bifurcation in parametrically driven trapped atoms, *Phys. Rev. A.* **68**, 031403 (2003).

161. K. Kim, H.-R. Noh, H.-J. Ha, and W. Jhe, Direct observation of the sub-Doppler trap in a parametrically driven magneto-optical trap, *Phys. Rev. A.* **69**, 033406 (2004).

162. K. Kim, H.-R. Noh, and W. Jhe, Measurements of trap parameters of a magneto-optical trap by parametric resonance, *Phys. Rev. A.* **71**, 033413 (2005).

163. K. Kim, M.-S. Heo, K.-H. Lee, K. Jang, H.-R. Noh, D. Kim, and W. Jhe, Spontaneous symmetry breaking of population in a nonadiabatically driven

Q. Baudouin, W. Guerin, and R. Kaiser

atomic trap: An ising-class phase transition, *Phys. Rev. Lett.* **96**, 150601 (2006).

164. D. Wilkowski, J. Ringot, D. Hennequin, and J. C. Garreau, Instabilities in a magneto-optical trap: Noise-induced dynamics in an atomic system, *Phys. Rev. Lett.* **85**, 1839–1842 (2000).

165. A. di Stefano, P. Verkerk, and D. Hennequin, Deterministic instabilities in the magneto-optical trap, *Eur. Phys. J. D.* **30**, 243–258 (2004).

166. R. Romain, D. Hennequin, and P. Verkerk, Phase-space description of the magneto-optical trap, *Eur. Phys. J. D.* **61**, 171–180 (2011).

167. M. Chalony, J. Barré, B. Marcos, A. Olivetti, and D. Wilkowski, Long-range gravitational-like interaction in a neutral atomic cold gas, *Phys. Rev. A.* **87**, 013401 (2013).

168. G. Labeyrie, F. Michaud, and R. Kaiser, Self-sustained oscillations in a large magneto-optical trap, *Phys. Rev. Lett.* **96**, 023003 (2006).

169. T. Pohl, G. Labeyrie, and R. Kaiser, Self-driven nonlinear dynamics in magneto-optical traps, *Phys. Rev. A.* **74**, 023409 (2006).

170. G.-L. Gattobigio, F. Michaud, G. Labeyrie, T. Pohl, and R. Kaiser, Light mediated long range interactions between neutral atoms, *AIP Conf. Proc.* **862**, 211 (2006).

171. D. H. E. Dubin and T. M. O'Neil, Computer simulation of ion clouds in a penning trap, *Phys. Rev. Lett.* **60**, 511–514 (1988).

172. A. B. Fokin, Semi-regular and alternating pulsations in hydrodynamical models for low-mass giants, *Astrophys. Space Sci.* **164**, 95–106 (1990).

173. A. Olivetti, J. Barré, B. Marcos, F. Bouchet, and R. Kaiser, Breathing mode for systems of interacting particles, *Phys. Rev. Lett.* **103**, 224301 (2009).

174. A. Olivetti, J. Barré, B. Marcos, F. Bouchet, and R. Kaiser, Breathing mode for systems of interacting particles in the microcanonical and canonical descriptions, *Transport Theor. Stat. Phys.* **39**, 524–551 (2010).

175. J. T. Mendonça, R. Kaiser, H. Terças, and J. Loureiro, Collective oscillations in ultracold atomic gas, *Phys. Rev. A.* **78**, 013408 (2008).

176. H. Terças, J. T. Mendonça, , and R. Kaiser, Driven collective instabilities in magneto-optical traps: A fluid-dynamical approach, *Europhys. Lett.* **89**, 53001 (2010).

177. L. Tonks, The high frequency behavior of a plasma, *Phys. Rev.* **37**, 1458–1483 (1931).

178. A. Dattner, Resonance densities in a cylindrical plasma column, *Phys. Rev. Lett.* **10**, 205–206 (1963).

179. C. Aerts, J. Christensen-Dalsgaard, and D. W. Kurtz, *Asteroseismology.* Springer (2010).

180. A. T. Black, H. W. Chan, and V. Vuletić, Observation of collective friction forces due to spatial self-organization of atoms: From Rayleigh to Bragg scattering, *Phys. Rev. Lett.* **91**, 203001 (2003).

181. K. Baumann, C. Guerlin, F. Brennecke, and T. Esslinger, Dicke quantum phase transition with a superfluid gas in an optical cavity, *Nature.* **464**, 1301–1306 (2010).

182. G. Labeyrie, E. Tesio, P. M. Gomes, G.-L. Oppo, W. J. Firth, G. R. M.

Robb, A. S. Arnold, R. Kaiser, and T. Ackemann, Optomechanical self-structuring in cold atomic gases, *Nature Photon.* **8**, 321–325 (2014).

183. J. Arons, Photon bubbles - overstability in a magnetized atmosphere, *ApJ.* **388**, 561–578 (1992).

184. C. F. Gammie, Photon bubbles in accretion discs, *Mon. Not. Roy. Astron. Soc.* **297**, 929–935 (1998).

185. N. J. Turner, E. Quataert, and H. W. Yorke, Photon bubbles in the circumstellar envelopes of young massive stars, *ApJ.* **662**, 1052 (2007).

186. J. T. Mendonça and R. Kaiser, Photon bubbles in ultracold matter, *Phys. Rev. Lett.* **108**, 033001 (2012).

187. R. Kaiser and M. D. Havey, Mesoscopic electromagnetic wave dynamics in ultracold atomic gases, *Opt. Photon. News.* **16**, 38–43 (2005).

188. G. Labeyrie, Coherent transport of light in cold atoms, *Mod. Phys. Lett. B.* **22**, 73–99 (2008).

189. R. H. Dicke, Coherence in spontaneous radiation processes, *Phys. Rev.* **93**, 99–110 (1954).

190. M. Gross and S. Haroche, Superradiance: an essay on the theory of collective spontaneous emission, *Phys. Rep.* **93**, 301–396 (1982).

191. M. O. Scully and A. A. Svidzinsky, The super of superradiance, *Science.* **325**, 1510–1511 (2009).

192. R. Friedberg, S. R. Hartmann, and J. T. Manassah, Frequency shifts in emission and absorption by resonant systems of two-level atoms, *Phys. Rep.* **3**, 101–179 (1973).

193. M. O. Scully and A. A. Svidzinsky, The Lamb shift – yesterday, today, and tomorrow, *Science.* **328**, 1239–1241 (2010).

194. T. Bienaimé, S. Bux, E. Lucioni, P. W. Courteille, N. Piovella, and R. Kaiser, Observation of cooperative radiation pressure in presence of disorder, *Phys. Rev. Lett.* **104**, 183602 (2010).

195. T. Bienaimé, N. Piovella, and R. Kaiser, Controlled Dicke subradiance from a large cloud of two-level systems, *Phys. Rev. Lett.* **108**, 123602 (2012).

196. J. R. Ott, M. Wubs, P. Lodahl, N. A. Mortensen, and R. Kaiser, Cooperative fluorescence from a strongly driven dilute cloud of atoms, *Phys. Rev. A.* **87**, 061801(R) (2013).

197. A. Biella, F. Borgonovi, R. Kaiser, and G. L. Celardo, Subradiance localization in the open 3D Anderson-Dicke model, *Europhys. Lett.* **103**, 57009 (2013).

198. P. F. Bedaque, H. Caldas, and G. Rupak, Phase separation in asymmetrical fermion superfluids, *Phys. Rev. Lett.* **91**, 247002 (2003).

199. J. M. Gerton, D. Strekalov, I. Prodan, and R. G. Hulet, Direct observation of growth and collapse of a Bose–Einstein condensate with attractive interactions, *Nature.* **408**, 692–695 (2000).

200. E. A. Donley, N. R. Claussen, S. L. Cornish, J. L. Roberts, E. A. Cornell, and C. E. Wieman, Dynamics of collapsing and exploding Bose–Einstein condensates, *Nature.* **412**, 295–299 (2001).

201. L. J. Garay, J. R. Anglin, J. I. Cirac, and P. Zoller, Sonic analog of gravitational black holes in Bose-Einstein condensates, *Phys. Rev. Lett.* **85**,

62   *Q. Baudouin, W. Guerin, and R. Kaiser*

     4643–4647 (2000).

202. S. Giovanazzi, Hawking radiation in sonic black holes, *Phys. Rev. Lett.* **94**, 061302 (2005).

203. O. Lahav, A. Itah, A. Blumkin, C. Gordon, S. Rinott, A. Zayats, and J. Steinhauer, Realization of a sonic black hole analog in a Bose-Einstein condensate, *Phys. Rev. Lett.* **105**, 240401 (2010).

204. C. Barceló, S. Liberati, and M. Visser, Analogue gravity from Bose-Einstein condensates, *Class. Quantum Grav.* **18**, 1137 (2001).